RC beams under blast load: reliability and sensitivity analysis

Flavio Stochino[1]

Department of Architecture Design and Urban Planning, University of Sassari, Asilo Sella, via Garibaldi 35, 07041 Alghero (SS), Italy, fstochino@uniss.it

abstract

The effects of blast loading on structures can be very dangerous: damages and failures are expected with serious threats to structural safety and human life. Materials stresses and strains are often pushed to the limit and the modelling of these phenomena can be very complex. In order to design blast-resistant structures it is very important to determine what are the key parameters of this problem.
This paper presents a reliability and parametric analysis of the response of Reinforced Concrete (RC) beams under blast loads. The main aim is to highlight the key parameters of the problem in order to produce information useful for the design of reliable blast-resistant RC structures.
The beam has been idealised as an equivalent SDOF system, in which strain-rate effects are accounted for. This approach is convenient from a computational point of view and it has been validated by a direct comparison with a more sophisticated finite element model and with experimental results found in literature. Then a sensitivity analysis of the parameters involved in beam response under blast load has been developed. Slenderness (which has a direct effect on stiffness) and peak load prove to be the most important parameters, but span length (which has an important influence on the mass) is also a key parameter. Other variables such as concrete strength and reinforcement ratio do not seem to have a strong correlation with the beam response.

keywords

Structural failures, Explosion, Reliability analysis, Strain rate, Breaking load.

1 Introduction

Nowadays, the issue of structural safety under blast loading has become a dramatic problem. The tragic news of the terrorist attacks of recent years (9/11/2001, New York; 7/7/2005, London; 7/23/2005, Sharm El Sheik; 20/09/2008, Islamabad 1/24/2011, Moscow; etc), raise important, urgent questions regarding the real safety and reliability of our buildings. Extreme loads such as impacts, explosions, etc., can occur in everyday life with unexpectedly high frequency. Actually, the problem of terrorist attacks, so important for strategic and military building design, has been linked to residential and industrial building explosion accidents.

The effects of blast loading on structures can be very dangerous, damages and failures are expected with serious treats to structural safety and human life. Materials stresses and strains are often pushed to the limit and the modelling of these phenomena can be very complex. The peculiarities of damages induced by blast load can be treated as “fingerprints” and allow to estimate the load characteristics in a back analysis process. This issue is well presented in the review paper [1] where the explosion aftermath analysis can be synthetized by two main questions: what damage is

[1] Corresponding author.
Please cite this document as: STOCHINO F. “RC beams under blast load: Reliability and sensitivity analysis”, *Engineering Failure Analysis*, (2016) 66, 544-565. http://dx.doi.org/10.1016/j.engfailanal.2016.05.003

seen? What does the damage mean? In this way, important lessons can be learned also by real case studies: for example in [2] the real blast-induced collapse of bridge is investigated. Its failure was due to a firework explosion and important information about the explosive charge and its real location were assessed looking at the damages.

As said before the structural response under blast load is not trivial. In the scientific literature several papers were devoted to the study of simple structural elements like beams and columns. The most elementary dynamic model consists of schematizing the beam with a Single Degree of Freedom (SDOF) system. This approach simplifies the theoretical formulation of the problem and its solution. It has a quite low computational cost but it usually requires the introduction of empirical formulas and, in addition, it does not provide full information on beam response.

A first example of this approach is reported in the pioneering work by Frankland [3] which presents an early, simple model: purely undamped elastic SDOF. In a quite recent paper, [4], Morison distinguishes two main SDOF approaches:

- Modal Method.

- Equivalent SDOF Method

The modal method was first presented in 1946 in the US Manual EM 1110-345-405, and, in 1965, re-issued as TM5-855-1 [5]. This method assumes that the elastic forced response of the real element is approximated by its first mode of free vibration. In case of elastic-pure plastic resistance function, the equation of motion can be solved in a closed-form, and referring to an idealised blast load, with triangular/rectangular time-history, maximum deflection can be easily calculated.

In the fifties, knowledge in this field increased, and the elastic-plastic model was considered. In an early work, Seiler et al. [6] modelled, by means of SDOF, a simply-supported beam under impulsive loading. They assumed that the initial velocity was a half sine wave. In this case, a simple mass-spring system can model the behaviour of elastic-plastic and rigid-plastic beams in order to develop a comparison between the two approaches. Then, Brooks and Newmark, in [7], investigated numerous dynamic structural problems. In particular, Newmark [8 - 9] was an influential proponent of the modal method, having calculated several modal period formulas and corresponding stiffness and strength expressions.

The equivalent SDOF method appeared in 1957 in the US Army Corps of Engineers manual: see [10 – 11]. This method relies on the calculation of SDOF parameters based on the equivalence of energy: the equivalent mass must have equal kinetic energy, the equivalent resistance must have equal internal strain energy and the equivalent loading must have equal external work to the real distributed element. These equivalent factors can be calculated for different structures with different boundary and loading conditions. A thorough presentation of this method is proposed in the well known Biggs book [12], which is a milestone for this kind of problems.

Most of recent SDOF models (see [13 – 17]) are based on the latter approach, their reduced computational time is a key characteristics that makes them very convenient, in comparison with more advanced numeric and analytic models, when it is necessary to develop an high number of dynamic analyses. However when it necessary to have more information on the beam response (e.g. time history of the distribution of displacements and curvature along the span) Multi Degree Of Freedom (MDOF) and continuous beam models are more effective: see [18 – 23] for Timoshenko beam theory, and [24] for Euler-Bernoulli beam theory.

Actually the development of numeric methods and in particular of Finite Element Analysis (FEA) has improved the reliability of this approach. In case of blast and impulsive loading a very efficient code is LS-Dyna which is considered as a standard for both concrete structures (e.g. [25 – 27]) and

Please cite this document as: STOCHINO F. “RC beams under blast load: Reliability and sensitivity analysis”, *Engineering Failure Analysis*, (2016) 66, 544-565. http://dx.doi.org/10.1016/j.engfailanal.2016.05.003 - © 2016. this manuscript version is made available under the CC-BY-NC-ND 4.0 license

steel structures (e.g. [28]). Furthermore some very interesting papers dealing with blast effects on glass structures and their design have been recently published by Amadio and Bedon: [29 – 31].

Experimental test of reinforced concrete elements subjected to blast load are of paramount relevance to set benchmark data necessary to validate the numerical model, however they are costly and difficult to carry out. In addition the spread of these results is often limited for defence purposes. Thus field results published in the international scientific literature are very important.

Magnusson et al. ([32 – 36]) subjected many reinforced concrete beams, with or without steel fibres, to air blast loading using a shock tube. One of the main important results is that the beams with a high reinforcement ratio and without steel fibres failed in shear, while those with a low reinforcement ratio failed in flexure. In addition, an explicit non-linear numerical model is developed in [37] with the aim of interpreting and describing the above mentioned experimental results. The effects of explosion on reinforced concrete beams strengthened by carbon fibres polymers was studied also in [38] by Hudson and Darwin.

It is important to mention also the experimental works by Remennikov et al [39], Fujikake et al [40], Zhan et al [41] and Tachibana et al [42], in which reinforced concrete beams under impact loads were investigated. In [43], Giovino et al subjected a set of RC panels to open-field blast in order to study the response of RC cladding under impulsive load due to external bomb. One way RC slab under blast load are also tested and modelled by FEA in [44].

An interesting study is presented in [45] were different strategies to strengthen RC elements are developed and tested with field experiment in order to prevent blast-induced failure, but very important results for close-in blast load are presented also in [46]. Indeed, in the latter work, an empirical scale law is proposed and it can be suitable for design purpose.

Blast load due to accidents or terroristic attacks cannot be forecasted in a deterministic way. Thus design procedures that consider explosion load must take into account the randomness of the threatening and of the load scenario. In addition, also the mechanical characteristics of materials cannot be assessed in a deterministic way and this is particularly important in case of RC structures. Therefore, when the randomness of these parameters is accounted for, the structural response assumes a probabilistic nature, making it necessary to look at reliability analysis. The probabilistic approach to structural reliability in the case of a blast load is a current topic in structural engineering. Due to the important computational effort to develop such kind of analysis the SDOF model becomes very convenient. For example in quite an early work [47], Low and Hao presented results from a parametric investigation of the reliability of reinforced concrete slabs under blast load. The authors considered an equivalent non-linear SDOF system, also taking into account the strain-rate effect. In [48], Rong and B. Li developed a probabilistic analysis of maximum displacement and ductility factors for a reinforced concrete flexural member under explosion load, using a non-linear dynamic analysis of its equivalent SDOF system. The Monte Carlo simulation method (see also [49]) was used in this paper, and the authors obtained two non-dimensional indices quantifying differences between real response and the one obtained by means of the SDOF model. An interesting sensitivity analysis was obtained by Borenstein and Benaroya in [50] in order to determine which parameter uncertainties have the greatest effect on the maximum deflection of a clamped aluminium plate subjected to a blast load. The Monte Carlo simulation was also used in this case. The authors took into account some blast-wave parameters such as loading duration time. Actually, they state that the response of the plate is most sensitive to the latter variable.

More recently in [51], Olmati et al. developed an interesting probabilistic analysis of precast RC panels under blast load developing fragility curves for different limit states. Fragility curves (see also [52 – 53]) are a powerful tool for non-deterministic studies. In this framework they represents

the probability of exceeding a given damage state (or performance) as a function of an engineering demand parameter that represents the blast load.

In this paper a reliability analysis of simple supported RC beams under blast load is developed with a non-linear equivalent SDOF model that is validated by comparison with experimental findings present in literature. The model, described in Section 2, takes into account materials constitutive laws sensitive to the strain rate and allows to analyse the effects of various parameters defining the load and the mechanical and geometrical characteristics of the beams. Thus a sensitivity analysis, based on least squares regression, is shown in Section 3. Its results, reported in Section 4, include some polynomial relationships that relate structural response in terms of maximum velocity and displacements to the characteristics of the load scenario. Some concluding remarks and prospective developments are stated in Section 5.

2. SDOF model

In the following paragraphs a synthetic presentation of the structural model used for the numerical analysis is given.

2.1 Materials models

The constitutive properties of concrete and steel, considered in the model, are defined in the following. Referring to fib Bulletin n. 55 [54], the uniaxial behaviour of reinforcing steel (both in tension and in compression) is approximated by an elastic-perfect plastic diagram, as shown in Fig. 1a ([54]§ 5.2.9). In this figure, E_s is the label for Young's steel modulus, f_{yk} denotes its yield strength and ε_{sy} represents its yield strain.

The uniaxial stress-strain relation of concrete is expressed by a rational function ([54],§ 5.1.8.1):

$$\sigma_c = f_{cm}\frac{k\cdot\frac{\varepsilon_c}{\varepsilon_{c1}}-\left(\frac{\varepsilon_c}{\varepsilon_{c1}}\right)^2}{1+(k-2)\cdot\frac{\varepsilon_c}{\varepsilon_{c1}}} \quad for|\varepsilon_c| < \left|\varepsilon_{c,lim}\right|, \tag{1}$$

where ε_c (<0) is concrete compressive strain, σ_c (<0) is concrete compressive stress, while f_{cm}, ε_{c1}, $\varepsilon_{c,lim}$ and k are a set of parameters which defines the concrete constitutive law (see Fig. 1b) depending on its grade ([54],Table 5.1-8). It is important to highlight that the tensile strength of concrete is disregarded.

Please cite this document as: STOCHINO F. "RC beams under blast load: Reliability and sensitivity analysis", *Engineering Failure Analysis*, (2016) 66, 544-565. http://dx.doi.org/10.1016/j.engfailanal.2016.05.003 - © 2016. this manuscript version is made available under the CC-BY-NC-ND 4.0 license

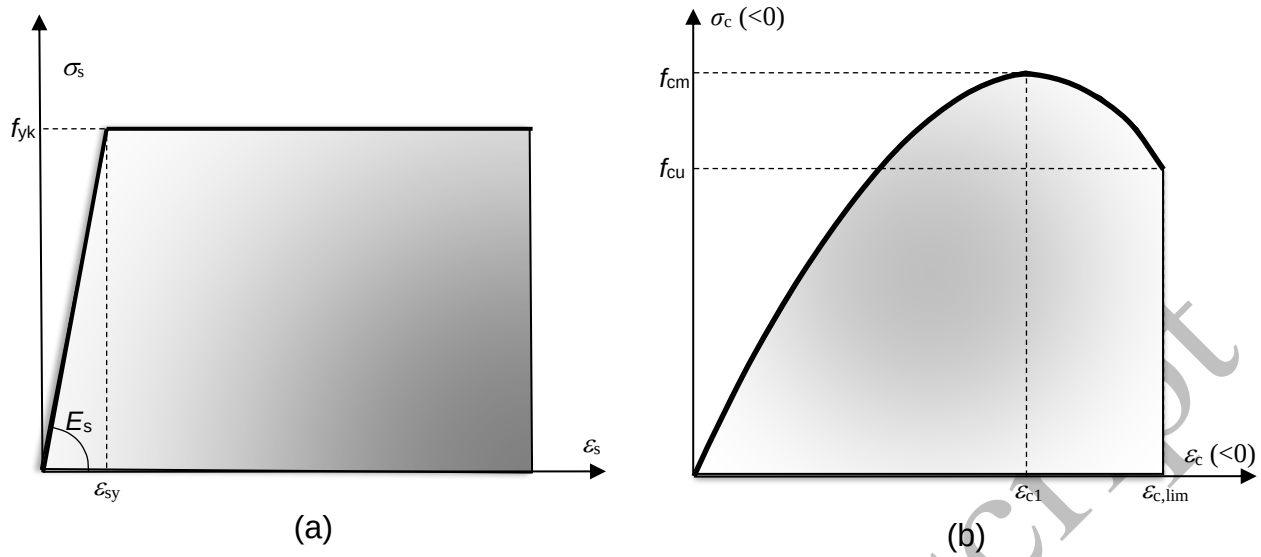

Fig. 1: Stress-strain diagrams for reinforcing steel (a) and concrete (b) assumed in this model.

2.2 Cross section model

In this model the yield state of the beam is identified by the tensile reinforcement yielding condition. The neutral axis depth at the yield state, denoted by x_y, can be obtained by imposing translational equilibrium (see Eq. (2)) while the corresponding bending moment M_y is defined by the rotational equilibrium expressed in Eq. (3).

$$b\int_0^{x_y}\sigma_c\,dy+\sigma_{ss}A_{ss}=f_{yk}A_s, \qquad (2)$$

$$M_y=b\int_0^{x_y}\sigma_c(d-y)\,dy+\sigma_{ss}A_{ss}(d-d'). \qquad (3)$$

Here the subscripts “s” and “ss” are appended to quantities respectively corresponding to tensile and compressive reinforcements, while the subscript “c” refers to concrete. The meanings of all geometric quantities relative to the beam cross-section can be inferred from Fig. 2.

Please cite this document as: STOCHINO F. “RC beams under blast load: Reliability and sensitivity analysis”, *Engineering Failure Analysis*, (2016) 66, 544-565. http://dx.doi.org/10.1016/j.engfailanal.2016.05.003 - © 2016. this manuscript version is made available under the CC-BY-NC-ND 4.0 license

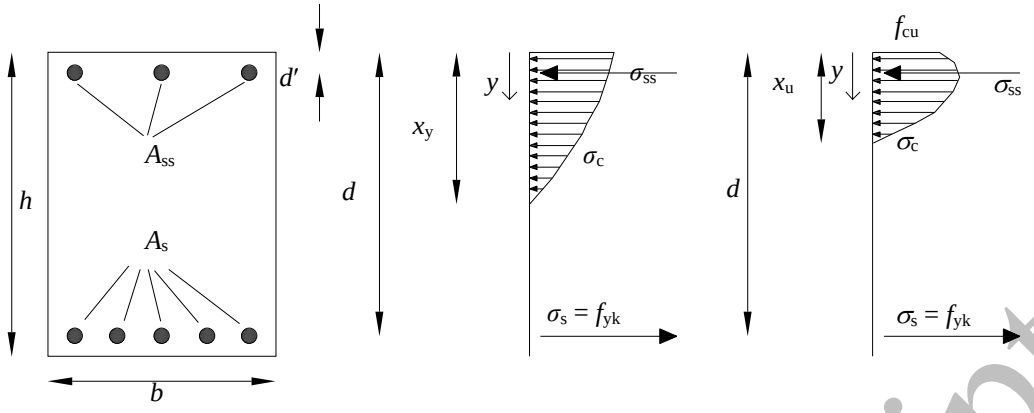

Fig. 2: (a) Sketch of the cross-section of a doubly-reinforced concrete beam; (b) stress diagram at the yield state; (c) stress diagram at the ultimate state.

The ultimate limit state is reached when concrete attains its maximum strain $\varepsilon_{c,lim}$. Stress distribution corresponding to this case is reported in Fig. 2c. Neutral axis depth at the ultimate state (x_u) can be calculated again from the translational equilibrium condition:

$$b\int_0^{x_u}\sigma_c\,dy+\sigma_{ss}A_{ss}=f_{yk}A_s, \tag{4}$$

The resistant bending moment at the ultimate state (M_u) can be expressed by rotational equilibrium around the tensile reinforcement:

$$M_u=b\int_0^{x_u}\sigma_c(d-y)\,dy+\sigma_{ss}A_{ss}(d-d'). \tag{5}$$

The bilinear bending moment-curvature diagram of the RC beam, illustrated in Fig. 3a can be obtained given the values of x_y, M_y, x_u and M_u. In the following, θ_y and θ_u represent curvatures at the yield and ultimate states, they are defined by:

$$\theta_y=\frac{\varepsilon_{sy}}{d-x_y}, \tag{6}$$

and

$$\theta_u=\frac{\varepsilon_{c,lim}}{x_u}, \tag{7}$$

respectively.

The nonlinear behaviour of a RC cross section, for an under-reinforced element, is often modelled by a bilinear relationship between bending moment and curvature. It is defined by the previously-

established characteristic points (yielding, ultimate). This approach is quite convenient from a computational point of view, but it hardly mimics the real behaviour of the RC cross section. Indeed it rarely exhibits a clear-cut transition between the elastic and plastic deformation fields. Thus, in this work, a smoother relationship between the bending moment M and curvature θ is assumed, which reads:

$$M = \bar{M}\tanh\left(\frac{\bar{K}}{\bar{M}}\theta\right) = -\bar{M}\tanh\left(\frac{\bar{K}}{\bar{M}}\frac{\partial^2 u}{\partial x^2}\right). \quad (8)$$

Eq.(8) introduce an hyperbolic tangent function because it presents no slope discontinuity and it is capable of fitting well also a bilinear function. The parameters $\bar{M}$ and $\bar{K}$, appearing in Eq.(8), depend on the sectional and constitutive properties of the beam. They respectively represent the equivalent ultimate bending moment and the initial flexural stiffness of the beam. For the sake of clarity, it should be highlighted that the right-hand term of Eq.(8) is obtained by assuming small deformation and rotation in the beam.

The parameter $\bar{K}$, which represents the slope of the diagram plotted in Fig. 3b at θ = 0, can be expressed by this ratio:

$$\bar{K} = \frac{M_y}{\theta_y}. \quad (9)$$

The equivalent ultimate bending moment $\bar{M}$, can be obtained by equating areas A_1 and A_2 under the curves shown respectively in Fig. 3a and in Fig. 3b. This equivalence yields:

$$\frac{\bar{M}^2}{\bar{K}}\ln\left[\cosh\left(\frac{\bar{K}}{\bar{M}}\theta_u\right)\right] = \frac{M_u(\theta_u - \theta_y) + M_y\theta_u}{2}, \quad (10)$$

where the left-hand term was obtained by integrating Eq.(8).
With this approach, the bilinear bending moment-curvature relationship can be substituted by a smoother diagram, which better approximates the actual behaviour of the beam.

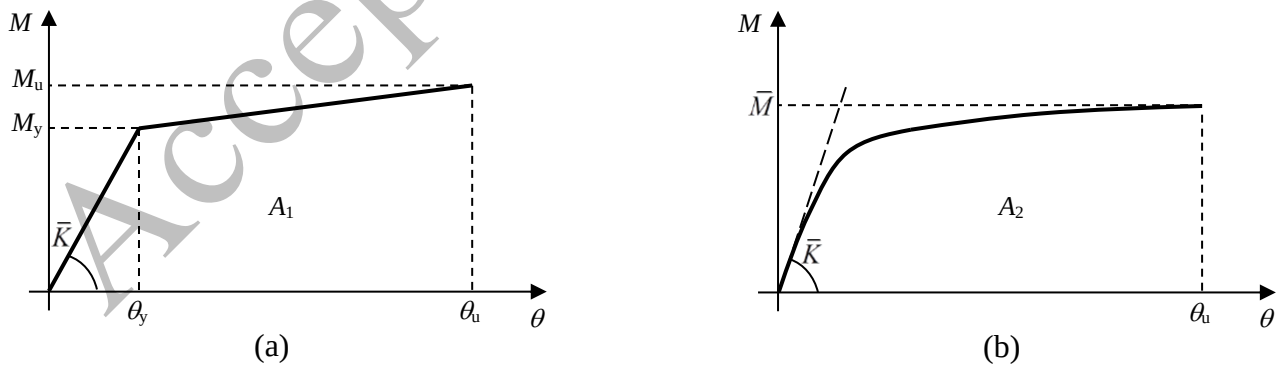

Fig. 3: (a) Bilinear bending moment-curvature relation; (b) smoother bending moment-curvature diagram adopted in this work.

Please cite this document as: STOCHINO F. “RC beams under blast load: Reliability and sensitivity analysis”, *Engineering Failure Analysis*, (2016) 66, 544-565. http://dx.doi.org/10.1016/j.engfailanal.2016.05.003 - © 2016. this manuscript version is made available under the CC-BY-NC-ND 4.0 license

2.3 Strain rate effects

Considering that concrete and steel are strain-rate sensitive materials and blast loading produces quite high strain rates the above-mentioned constitutive relationships, valid in quasi-static load case, must be modified in order to take into account strain rate effects. Thus the relationships provided by the *CEB Information Bulletin n.187* [55] are enforced in the model.
As a first step, the strain rates of concrete and steel reinforcements are determined by knowing the curvature rate and the value of the neutral axis depth. In the next step, the dynamic properties of concrete and steel reinforcements are evaluated. Concerning concrete ([55],§ 3.3.1), its dynamic strength is expressed by:

$$f_{cm,dyn} = f_{cm}\left(\frac{\dot{\varepsilon}_c}{30\cdot10^{-6}}\right)^{1.02\alpha} \quad if\ \dot{\varepsilon}_c \le 30\ s^{-1} \text{ a);}$$
$$f_{cm,dyn} = f_{cm}\gamma\dot{\varepsilon}_c^{\,1/3} \quad if\ \dot{\varepsilon}_c > 30\ s^{-1} \text{ b).} \qquad (11)$$

In Eqs. (11), $\dot{\varepsilon}_c$ is the strain rate of concrete, while $\alpha = 1/(5+3\cdot f_{cm}/4)$ and $\gamma = 10\text{^}(6.156\cdot\alpha - 0.492)$.

Concrete strains ε_{c1} and $\varepsilon_{c,lim}$ are augmented by the following expressions:

$$\varepsilon_{c1,dyn} = \varepsilon_{c1}\left(\frac{\dot{\varepsilon}_c}{30\cdot10^{-6}}\right)^{0.02}; \qquad (12)$$

$$\varepsilon_{c,lim,dyn} = \varepsilon_{c,lim}\left(\frac{\dot{\varepsilon}_c}{30\cdot10^{-6}}\right)^{0.02}. \qquad (13)$$

Concerning steel ([55],§ 3.4.2), its dynamic strength is calculated as:

$$f_{yk,dyn} = f_{yk}\left[1+\frac{6}{f_{yk}}\ln\left(\frac{\dot{\varepsilon}_s}{5\cdot10^{-5}}\right)\right] \quad if\ \dot{\varepsilon}_s \le 10\ s^{-1}\ , \qquad (14)$$

where $\dot{\varepsilon}_s$ is the strain rate of either tensile or compressive reinforcement. If $\dot{\varepsilon}_s$ > 10 s^{-1}, the limit value 10 s^{-1} is assigned to $\dot{\varepsilon}_s$ in Eq. (14). Instead, the longitudinal module of elasticity E_s is considered constant ([55], §3.4.3).

2.4 SDOF parameters

If the stand-off distance between the charge and the beam target is large enough the pressure wave due to the explosion can be considered uniform along the structural element surface. Fig. 4a, a simply supported beam subjected to a uniformly-distributed load is presented, while its equivalent SDOF system is sketched in Fig. 4b. It should be highlighted that damping is disregarded, since successive loading cycles are not considered; indeed, the first peak displacement is the most severe condition because it is unlikely the structure will collapse after unloading [56].

Please cite this document as: STOCHINO F. “RC beams under blast load: Reliability and sensitivity analysis”, *Engineering Failure Analysis*, (2016) 66, 544-565. http://dx.doi.org/10.1016/j.engfailanal.2016.05.003 - © 2016. this manuscript version is made available under the CC-BY-NC-ND 4.0 license

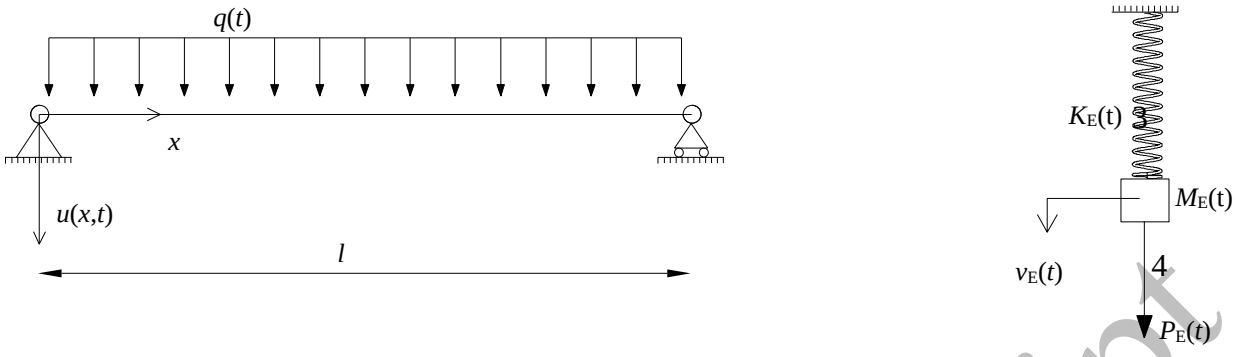

Fig. 4: (a) Real beam; (b) equivalent SDOF model of the real beam.

The elastic-plastic behaviour of the SDOF system can be represented by a bilinear load-displacement diagram, as shown in Fig. 5. The latter can be derived from the bending moment-curvature diagram of the beam (plotted in Fig. 3b), as described in the following:

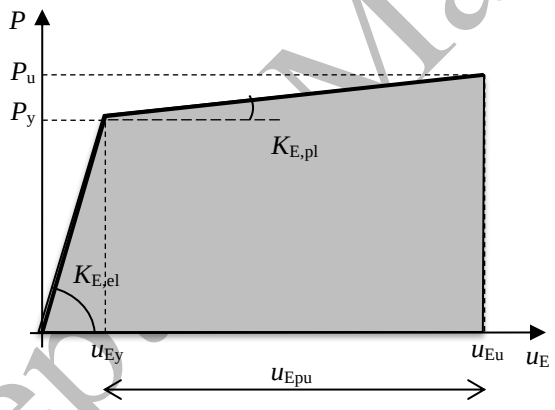

Fig. 5: bilinear load-displacement diagram of the equivalent SDOF model.

The rotational equilibrium equation defines the yield load P_y as a function of the yield bending moment M_y:

$$M_y = \frac{q_y \cdot l^2}{8} \quad \Rightarrow \quad P_y = q_y \cdot l = \frac{8 \cdot M_y}{l}, \tag{15}$$

where q_y is the uniformly-distributed load acting on the beam in the yield state. Yield displacement v_{Ey} is defined by means of the linear elastic theory of beams:

$$u_{Ey} = \frac{5 \cdot q_y \cdot l^4}{384 \cdot \bar{K}} = \frac{5 \cdot P_y \cdot l^3}{384 \cdot \bar{K}}, \tag{16}$$

where $\bar{K} = M_y/\theta_y$ is the elastic bending rigidity of the beam (see Fig. 3). Thus, the elastic stiffness of the SDOF system is given by:

Please cite this document as: STOCHINO F. "RC beams under blast load: Reliability and sensitivity analysis", *Engineering Failure Analysis*, (2016) 66, 544-565. http://dx.doi.org/10.1016/j.engfailanal.2016.05.003 - © 2016. this manuscript version is made available under the CC-BY-NC-ND 4.0 license

$$K_{E,el} = \frac{P_y}{v_{Ey}} = \frac{384 \cdot \bar{K}}{5 \cdot l^3}. \quad (17)$$

Equilibrium conditions can be enforced to obtain the ultimate load P_u:

$$M_u = \frac{q_u \cdot l^2}{8} \quad \Rightarrow \quad P_u = q_u \cdot l = \frac{8 \cdot M_u}{l}, \quad (18)$$

where q_u is the uniformly-distributed load on the beam at the ultimate state. The ultimate displacement, denoted by u_{Eu}, is evaluated by assuming a purely flexural failure: a concentrated plastic hinge is formed at the mid-span section of the beam, as depicted Fig. 6a. The plastic rotation after the generation of the plastic hinge is represented by φ_p, while u_{Ep} denotes the corresponding plastic displacement at the mid-span section. At the ultimate state $\varphi_p = \varphi_{pu}$, hence total plastic displacement, $u_{Ep} = u_{Epu}$ can be calculated as:

$$u_{Epu} = \frac{\varphi_{pu}}{2} \cdot \frac{l}{2} \, . \quad (19)$$

The ultimate displacement u_{Eu} can be obtained by introducing plastic hinge length l_p (Fig. 6b) and by denoting total plastic curvature by θ_p ($\theta_p = \theta_u - \theta_y$), assumed to be constant over l_p:

$$u_{Eu} = u_{Ey} + u_{Epu} = u_{Ey} + \frac{\varphi_{pu}}{2} \cdot \frac{l}{2} = u_{Ey} + \frac{\theta_p l_p}{2} \cdot \frac{l}{2} = u_{Ey} + \frac{1}{4}(\theta_u - \theta_y) l_p l \, . \quad (20)$$

Thus, plastic stiffness of the SDOF system is given by:

$$K_{E,pl} = \frac{P_u - P_y}{u_{Eu} - u_{Ey}}. \quad (21)$$

Unfortunately the plastic hinge length l_p cannot be determined *a priori*, but many approximate expressions for l_p are available in the literature. Here, the simple formula provided by Mattock (see [57]), is adopted:

$$l_p = d + 0.05 \cdot l. \quad (22)$$

For the sake of clarity it is important to point out that the effective height d is defined in the previous Fig. 2 and l is the beam span.

Please cite this document as: STOCHINO F. “RC beams under blast load: Reliability and sensitivity analysis”, *Engineering Failure Analysis*, (2016) 66, 544-565. http://dx.doi.org/10.1016/j.engfailanal.2016.05.003 - © 2016. this manuscript version is made available under the CC-BY-NC-ND 4.0 license

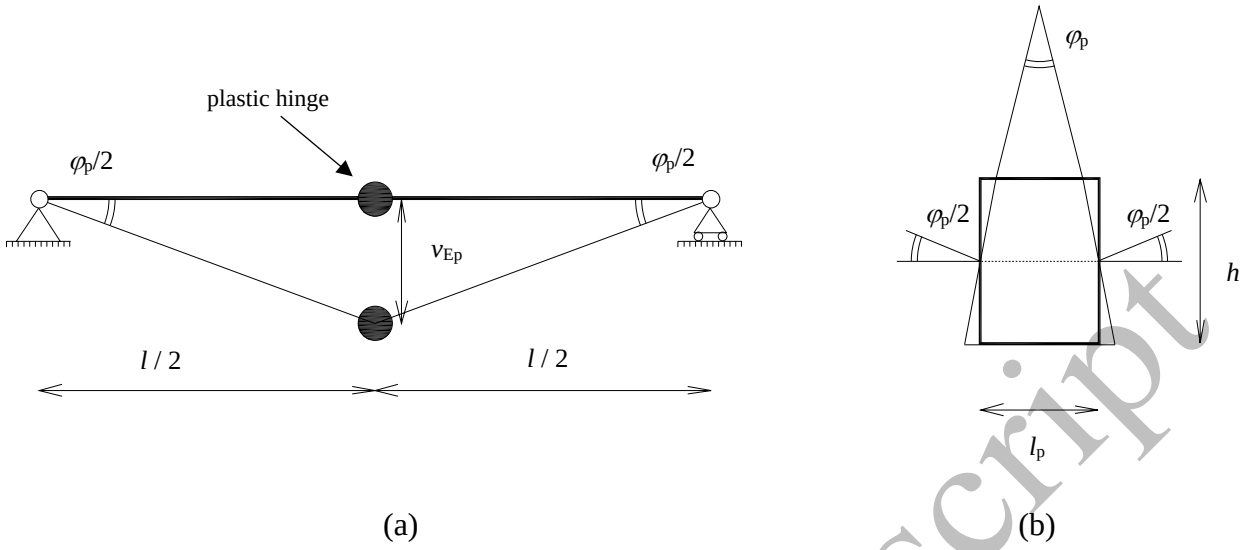

Fig. 6: (a) Plastic deflections of the beam with a concentrated plastic hinge at the mid-span section; (b) schematic representation of the plastic hinge.

2.5 SDOF motion equations

The non linear dynamic behaviour of the SDOF model under an external dynamic force P_E is described by the following set of ordinary differential equations (refer to Fig. 4 and Fig. 5):

$$M_{E,el}\frac{d^2u_E(t)}{dt^2} + K_{E,el}(t)u_E(t) = P_E(t) \qquad for\ 0 \le u_E \le u_{Ey} \qquad a); \tag{23}$$

$$M_{E,pl}\frac{d^2u_E(t)}{dt^2} + K_{E,pl}(t)u_E(t) + \left(K_{E,el}(t) - K_{E,pl}(t)\right)u_{Ey} = P_E(t) \qquad for\ u_{Ey} < u_E \le u_{Eu} \qquad b).$$

It is important to highlight that elastic and plastic stiffness ($K_{E,el}$ and $K_{E,pl}$) depends on time *t*, since the materials mechanical characteristics must be updated at each step of the calculation due to strain rate effects, as denoted in Section 2.3.
The equivalent load P_E is simply given by $P_E = q \cdot l$. A "load-mass factor" is necessary to define the elastic and plastic equivalent masses ($M_{E,el}$ and $M_{E,pl}$), it depends both on the type of regime (either elastic or plastic) and on the beam supports and loads. Thus the equivalent masses are obtained by multiplying the total mass of the beam (M_b) by the above mentioned factor; in particular, for a simply-supported beam with a uniformly distributed load, $M_{E,el} = 0.78 \cdot M_b$ and $M_{E,pl} = 0.66 \cdot M_b$ (see [12], Table 5.1).

2.6 Strain rate effects for the SDOF system

Since the dynamic properties of the materials are given in terms of their strain rates (see Eqs. (11)-(14)), it is necessary to relate the SDOF characteristics to material strain time history.

By solving Eq. (23) it is possible to evaluate the equivalent displacement u_E and equivalent velocity $\dot{u}_E = du_E/dt$ at each time step. Then the curvature θ_E and the curvature rate $\dot{\theta}_E = d\theta_E/dt$ at the mid-span section of the associated beam must be calculated. In the elastic regime, θ_E and $\dot{\theta}_E$ are obtained from linear elastic theory; in particular, for a simply-supported beam with a uniformly distributed load, they are given by:

$$\begin{aligned} \theta_E &= \frac{48 \cdot u_E}{5 \cdot l^2} \quad for\ 0 \le u_E \le u_{Ey} \quad a); \\ \dot{\theta}_E &= \frac{48 \cdot \dot{u}_E}{5 \cdot l^2} \quad for\ 0 \le u_E \le u_{Ey} \quad b). \end{aligned} \tag{24}$$

Instead, in the plastic regime it is supposed that a concentrated plastic hinge is formed at the mid-span section of the beam, as shown Fig. 6a. Thus, in this case θ_E and $\dot{\theta}_E$ can be evaluated by means of the following equations:

$$\begin{aligned} \theta_E &= \theta_y + \frac{\varphi_p}{l_p} = \theta_y + 2 \cdot \frac{u_{Ep}}{\frac{l}{2}} \cdot \frac{1}{l_p} = \theta_y + 2 \cdot \frac{u_E - u_{Ey}}{\frac{l}{2}} \cdot \frac{1}{l_p} \quad for\ u_{Ey} < u_E \le u_{Eu} \quad a); \\ \dot{\theta}_E &= 2 \frac{\dot{u}_E}{l/2} \cdot \frac{1}{l_p} \quad for\ u_{Ey} < u_E \le u_{Eu} \quad b). \end{aligned} \tag{25}$$

At each step of the calculation, the value of θ_E (given by either Eq. (24) or Eq. (25)) allows to determine the value of the bending moment M from the bending moment-curvature diagram in Fig. 3b. Then, the rotational equilibrium yields the neutral axis depth (here denoted as $\bar{x}$). Consequently, the strain rates of concrete and of tensile and compressive steel reinforcements are calculated using the following expressions:

$$\begin{aligned} \dot{\varepsilon_c} &= \dot{\theta}_E \cdot \bar{x} \quad a); \\ \dot{\varepsilon_s} &= \dot{\theta}_E \cdot (d - \bar{x}) \quad b); \\ \dot{\varepsilon_{ss}} &= \dot{\theta}_E \cdot (\bar{x} - d') \quad c). \end{aligned} \tag{26}$$

The absolute values of the strain rates given by Eqs. (26) are introduced into Eqs. (11)-(14) to update the properties of the materials.

2.6 Model validation

The numerical procedure based on finite difference used for solving Eqs. (23) is here briefly sketched.

As a first step the static mechanical characteristics (bending moment and neutral axis depth at yield and ultimate states) are evaluated using Eqs. (2) - (5). Then the SDOF parameters $K_{E,El}$, $K_{E,pl}$, u_{Ey}, u_{Eu} are calculated using Eqs. (15)-(21). For each time step t a loop is developed in which the following variables are determined: vertical displacement u, obtained by solving Eqs. (23) by means of the Finite Difference Method[2] (null initial conditions are imposed, because the beam is at rest before the explosive charge is detonated) ; curvature $\theta = -\partial^2 u/\partial x^2$ and the curvature

[2] The derivatives are approximated with finite differences of the 2nd order accuracy. Convergence studies have shown that a good choice of the time step is 10^{-5} s.

Please cite this document as: STOCHINO F. "RC beams under blast load: Reliability and sensitivity analysis", *Engineering Failure Analysis*, (2016) 66, 544-565. http://dx.doi.org/10.1016/j.engfailanal.2016.05.003 - © 2016. this manuscript version is made available under the CC-BY-NC-ND 4.0 license

rate $\dot{\theta} = \partial\theta/\partial t$ (enforcing Eq. (24) or (25)); bending moment M corresponding to curvature θ from Eq. (8);; neutral axis depth from rotational equilibrium under the applied bending moment M; strains of concrete and steel reinforcements using the linear deformation diagram and curvature value;; strain rates of concrete and steel reinforcements. Then the mechanical characteristics of materials are updated by means of Eqs. (11)-(14) and consequently the values of K and M are modified for a particular time step t. The loop is closed when the collapse criterion, which has been defined as the attainment of maximum concrete strain (ultimate state), is satisfied.

A Finite Element (FE) model has been developed by means of commercial software with the aim of an accurate comparison with the SDOF model results. In particular, it is based on the fibre model consisting of dividing the cross-section of the beam into concrete fibres and steel rebars.

The fibre model is developed through the flexibility method (see [58]): assuming the equilibrium condition, the forces trend in the cross section are related to nodal forces by means of specific interpolation functions. The section constitutive law represents the link between strains and stress and a simple application of the principle of virtual forces leads to the matrix of flexibility.

The flexibility method has several advantages in case of nonlinear analysis: the force interpolation matrix is exact with any material constitutive behaviour and so it is not an approximation also in the plastic realm. Furthermore equilibrium considerations can easily produce additional force interpolation functions.

As concerns material models, a trilinear relationship between stress and strain is used for concrete, approximating with great precision the compressive stress-strain diagram shown in Fig. 1b (the tensile strength of concrete is however disregarded, in according to the assumptions of this work); for steel rebars, an elastic–perfectly plastic stress-strain diagram is adopted see Fig. 1a.

Lastly, it should be underlined that, since the software does not include a failure criterion for concrete crushing, the time-history provided by the FE solution is interrupted at the instant in time in which maximum concrete strain obtained from the SDOF model is reached.

In order to validate the SDOF model its theoretical results are compared with the FE ones and with the experimental findings obtained by Magnusson and Hallgren [33], who tested several simply-supported RC beams under shock waves produced in a shock tube. The explosive charge was located far enough from the beam to generate a plane wavefront, hence a uniformly-distributed load.

Beam label	**B40-D5**
span length	1.500 m
width of cross-section	0.300 m
depth of cross-section	0.160 m
concrete cover	0.025 m
tensile reinforcement	5 ϕ16 mm
compressive reinforcement	2 ϕ 10 mm
concrete compressive strength	43 MPa
maximum concrete strain registered	3.69 ‰
steel yield strength	604 MPa
steel elastic modulus	210 GPa
mass per unit length	120 kg/m

Table 1: Properties of the beam labelled B40-D5 (extrapolated from [33]).

The beam labelled B40-D5 is examined and its characteristics are reported in Table 1, while the load time-history recorded during the experiment is reported in Fig. 7. The parameter chosen to

compare experimental data with theoretical results is midspan deflection, obviously representing maximum deflection, henceforth indicated by u_{max}.
The FE model mesh is consistent with the ones used for the SDOF finite difference integration scheme: the time step is 10^{-6} s and the space step is 0.05 m which corresponds to 30 beams elements for this case. The author has selected this value after a convergence study on the element lengths given the time step.

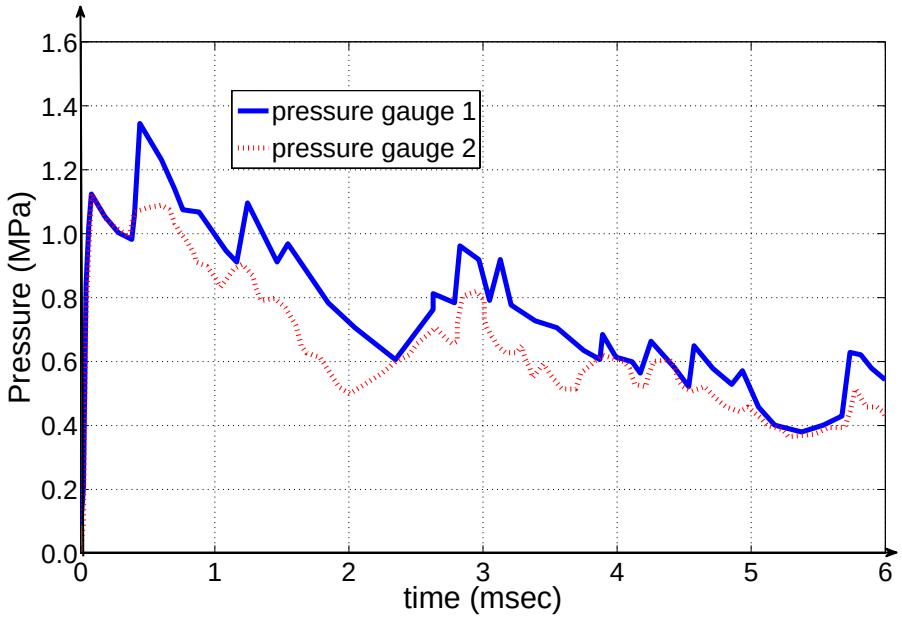

Fig. 7: Load time-history for beam labelled B40-D5, (extrapolated from [33]).

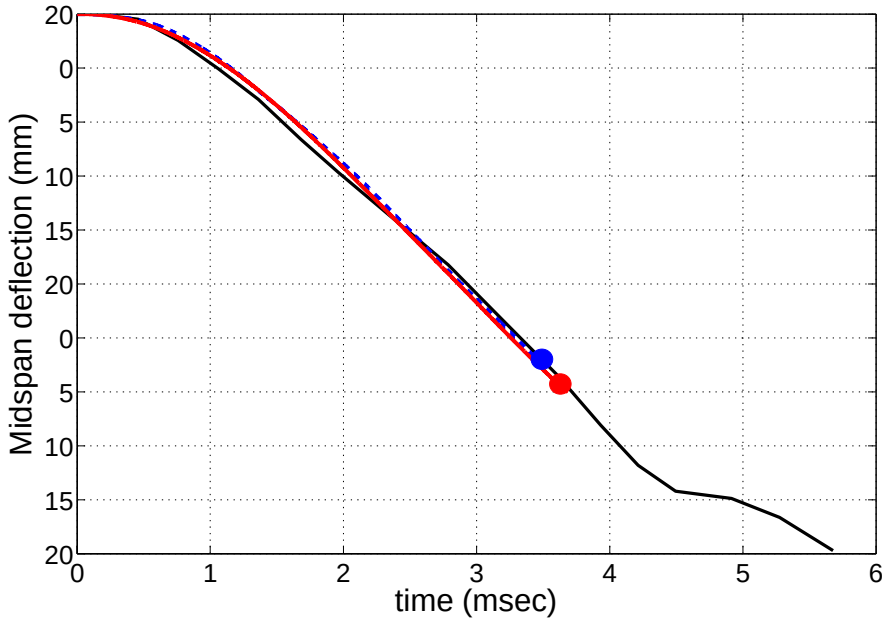

Fig. 8: Midspan deflection for beam labelled B40-D5, the red continuous line represents the SDOF results, the dotted blue ones corresponds to the FE model and the black one denotes the experimental finding. The circular spot highlight the failure condition.

The experimental time-history of beam midspan displacement u_{max} is plotted with a solid black line in Fig. 8. The red solid curve represents the SDOF model prediction and the dotted blue one denotes the FE results. Both models have produced quite accurate results in agreement with the

Please cite this document as: STOCHINO F. "RC beams under blast load: Reliability and sensitivity analysis", *Engineering Failure Analysis*, (2016) 66, 544-565. http://dx.doi.org/10.1016/j.engfailanal.2016.05.003 - © 2016. this manuscript version is made available under the CC-BY-NC-ND 4.0 license

experiments. The circular spots represent the models failure condition which it is not easily detectable in the field data. Indeed, the displacements transducers keep on recording even if the beams is beyond its ultimate limit state. However, it is important to highlight that the last part of the experimental curve exhibits an abrupt change, which can be attributed either to a small damage of the experimental apparatus or, more probably, to the crushing of concrete.
The results presented in Fig. 8 proves the accuracy of the SDOF model and allow to consider it as a reliable tool for the sensitivity analysis developed in the next Section.

3. Sensitivity Analysis

In order to design blast-resistant structures it is essential to determine the key parameters in this kind of problems. For this reason, a sensitivity analysis is developed in this paper. Numerical simulations by means of the above presented SDOF model are developed, considering different load scenarios and beam characteristics. This model was chosen because it is very convenient from a computational point of view. As it will become clear in the following paragraphs the need of short computational time is of fundamental importance in this analysis.
After a first reliability assessment necessary to detect a set of beams that has withstood the blast load, a sensitivity analysis is developed considering only it. The base idea is to look for any correlations between the response of the SDOF and the different parameters defining the dynamic problem: peak load, slenderness, span length, etc. These correlations are detected looking at the least squares interpolation function that better fit the numerical data. The response of the SDOF is expressed by the maximum beam displacement (midspan deflection) and the corresponding velocity which can influence strain rates and, consequently, the mechanical characteristics of materials.

3.1 Load and geometrical/strength characteristics

The beams considered in the simulations are simply supported, and their geometrical/strength characteristics vary randomly within the limits reported in Table 2. In this way, it is possible to consider a wider range of solutions referring to the most common real cases.

Characteristic	Value
Span	6÷12 m
Slenderness L/h	9÷15
Width	h/2.5 m
$\rho_s = A_s/bd$	0.005÷0.01
$\rho_{As} = A_{ss}/A_s$	0.25÷0.5
Concrete	f_{ck}=20÷40 MPa
Steel	f_{yk}=450 MPa

Table 2: Geometrical and strength characteristics of beams with their variation range.

An uniform distributed dynamic load is applied to the beams. In order to represent an hemispherical detonation its time history is a triangle with a peak load varying from 100 to 800 kN and a positive phase duration within the range 2.7 – 5.0 msec.

3.2 Reliability Analysis

4000 runs of the SDOF model were performed. For the sake of clarity it is important to remember that the collapse criterion is always the same considered in the previous sections and it corresponds to the attainment of the ultimate concrete strain. A summary of the ultimate state check is shown in Fig. 9, which presents the failure percentage for the various slenderness values as a function of the peak load value. Indeed, considering that for flexural models beam stiffness is strictly dependent on the slenderness *(L/h)*, the reference to this parameter appears straightforward. For peak loads lower than 400 kN the collapse percentage is quite low for all slenderness smaller than 13. Indeed, the largest amount of beams failed for peak loads higher than 700 kN, only thick beams (*L/h*=9-10) can resist without failure. Taking into account these results, in order to study the effects of several parameters in the structural response, the loading condition was divided in two different cases: high load and low load, (see Fig. 9 and Fig. 10). The former is defined by a peak load *P* randomly varying between 0.8-0.4·10^6 N and positive phase duration between 2.7 and 5 msec, the latter by a peak pressure between 0.4 and 0.1·10^6 N and positive phase duration within the same limits.

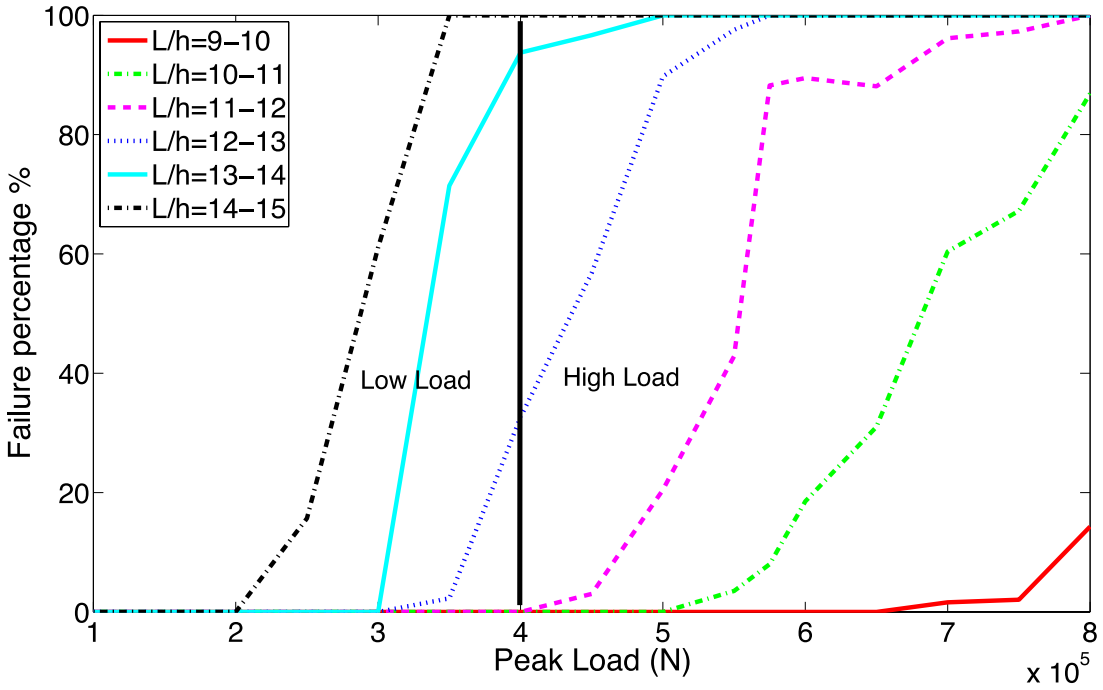

Fig. 9: Collapse percentage of the beams examined for different slenderness values. The solid black line distinguishes the low load from the high load case.

These scenarios can roughly represent a hemispherical above ground detonation of 55 kg of TNT with a stand off distance equal to 12 m (corresponding to low load scenario) or to 9 m (corresponding to high load scenario).

Please cite this document as: STOCHINO F. "RC beams under blast load: Reliability and sensitivity analysis", *Engineering Failure Analysis*, (2016) 66, 544-565. http://dx.doi.org/10.1016/j.engfailanal.2016.05.003 - © 2016. this manuscript version is made available under the CC-BY-NC-ND 4.0 license

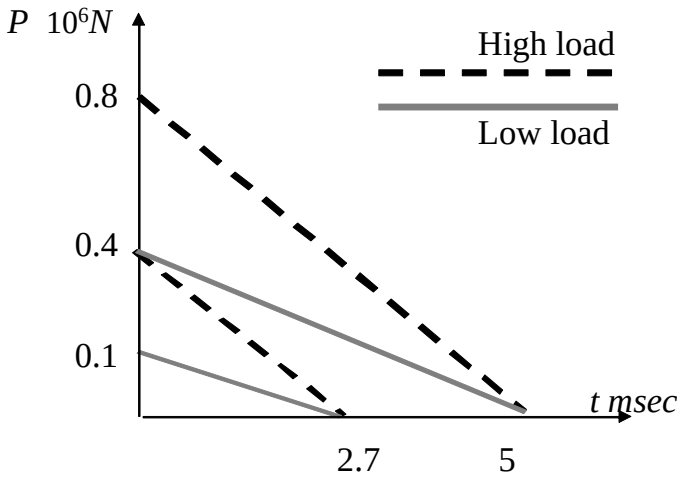

Fig. 10: Time-histories of the two load conditions: low and high.

The sensitivity analysis will be developed in the next paragraph considering the beams that are not collapsed in order to explore the effects of blast load on the maximum displacement and on the maximum velocity of each element.

3.3 Quality of fitting indicators

In the following Section 4, a thorough analysis will be developed considering various fitting models representing different relationships between variables of this problem. In order to quantitatively evaluate the quality of fitting, it is necessary to define some statistical parameters:

- Sum of Squares Due to Error: it is simply the sum of the squared difference between response value y_i and the predicted response value $\hat{y}_i$ (see Eq. (27)).

$$SSE = \sum_{i=1}^{n} (y_i - \hat{y}_i)^2 \quad (27)$$

- R-Square: it is an index representing how the fitting functions explains variation in data. It is defined in Eq. (30) as the ratio between the sum of squares regarding the mean $\bar{y}$ of regression (Eq. (28)) and the sum of squares regarding the mean $\bar{y}$ of the response value (see Eq. (29)). Due to its definition, R-Square assumes values between zero and one. A value equal to 0.72 means that fit explains 72% of the total variation in data as regards the average. For this reason, the best fits have higher R-Square values.

$$SSR = \sum_{i=1}^{n} (\hat{y}_i - \bar{y})^2, \quad (28)$$

$$SST = \sum_{i=1}^{n} (y_i - \bar{y})^2, \quad (29)$$

$$R_{\_SQUARE} = \frac{SSR}{SST}. \quad (30)$$

Please cite this document as: STOCHINO F. “RC beams under blast load: Reliability and sensitivity analysis”, *Engineering Failure Analysis*, (2016) 66, 544-565. http://dx.doi.org/10.1016/j.engfailanal.2016.05.003 - © 2016. this manuscript version is made available under the CC-BY-NC-ND 4.0 license

- Adjusted R-square: (AR-square) it is an optimal indicator of fitting validity when it is necessary to compare different models with different numbers of coefficients. If the residual degrees of freedom v are defined as the difference between response values m and fitted coefficients h, estimated from response values (see Eq (31)), the AR-square is defined by Eq. (32) and can have only a value less than or equal to one. Models with AR-square near 1 are better. There is the possibility of negative values; in this case, it means that the model contains terms that do not help in predicting response.

$$v = h - m, \tag{31}$$

$$AR_{\_SQUARE} = 1 - \frac{SSE(h-1)}{SST(v)}. \tag{32}$$

- Root Mean Squared Error: it is a measure of the standard deviation of the random component in the data. It is defined by Eq. (33) and values closer to zero mean that the model fits well the SDOF results.

$$RMSE = \sqrt{SSE/v}. \tag{33}$$

4 Results

4.1 Two-dimensional relationships

In this paragraph, the influence of three variables is discussed: span length, slenderness and peak load. Indeed, given the slenderness the span length corresponds to the mass of the beam and, in impulsive load regime, it is crucial to determine the initial velocity[3]. Furthermore, the slenderness is strictly linked to the beam flexural stiffness and the peak load is a key parameter to identify the load.

For each case a polynomial least square interpolation is proposed evaluating the coefficients for a linear, quadratic, cubic and quartic fitting functions, reported respectively in Eqs. (34) - (37):

$$y = a_1 x + a_0, \tag{34}$$

$$y = a_2 x^2 + a_1 x + a_0, \tag{35}$$

$$y = a_3 x^3 + a_2 x^2 + a_1 x + a_0, \tag{36}$$

$$y = a_4 x^4 + a_3 x^3 + a_2 x^2 + a_1 x + a_0. \tag{37}$$

[3] If I, is the impulse and M is the equivalent mass of the beam, its initial velocity is I/M.

Function	SSE (m^2)	R-square	AR-square	RMSE (m)
Cubic Slend	0.9550	0.2918	0.2895	0.03204
Quadratic Slend	0.9562	0.2909	0.2893	0.03205
Quartic Slend	0.9548	0.2919	0.2889	0.03206
Linear Span	0.9585	0.2892	0.2884	0.03207
Quadratic Span	0.9576	0.2898	0.2883	0.03207
Linear Slend	0.9583	0.2893	0.2886	0.03207
Cubic Span	0.9574	0.2900	0.2877	0.03208
Quartic Span	0.9569	0.2903	0.2873	0.03209
Quadratic P.Load	1.2630	0.06364	0.0616	0.03683
Linear P.Load	1.2650	0.06206	0.0610	0.03684
Cubic P.Load	1.2620	0.06400	0.0610	0.03684
Quartic P.Load	1.2610	0.06504	0.0610	0.03684

Table 3 : Fitting performances for high-load maximum deflection results.

In order to discover the influence of these variables, Fig. 11-Fig. 14 have been prepared. The correlations between maximum deflection or velocity (obtained by SDOF during numerical simulations) and span length, slenderness and peak load are investigated.

It is important to distinguish between high-load and low-load conditions. In the former case, the number of non-collapsed beams is greatly inferior as compared to the case of low load.

Table 3 presents the fitting performance for the maximum deflection results of various polynomial functions of the above mentioned independent parameters (span length, slenderness and peak load). The general trend in these results is that the SSE index decrease as the number of model coefficients increases, while the best RMSE is obtained for the cubic function taking into account correlations between displacement and slenderness (see Fig. 11).

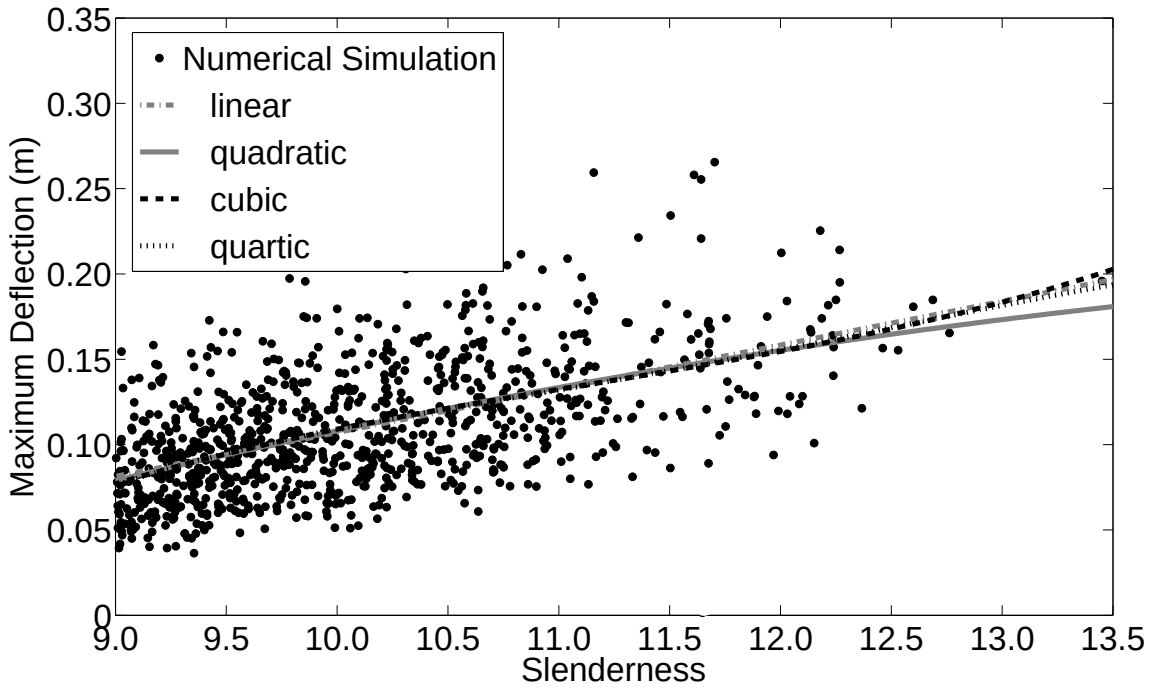

Fig. 11: High Load, Max. Def. – Slenderness different kinds of polyn. fittings.

It is important to highlight (referring to the results presented in Fig. 9) that almost all beams with slenderness greater than 12 and peak load greater than 6 10^5 N have failed. Hence, the influence of

these two important parameters is inferior as compared to what happens in the case of low load. In other words, only beams with a narrow range of slenderness (9-11) and peak-load variation (4-7·10^5 N) can be considered in the analysis. For this reason, the influence of span length is quite important in the case of high load and less significant in the other load condition. Regarding the latter correlation (maximum displacement and span length) the AR-square and RMSE best values correspond to the linear model; the adding of other coefficients to the model does not produces any improvement in fitting quality.

Thus, for the maximum displacement analysis in case of high-load, slenderness is the most important parameter, while the variation of peak load (within the above mentioned limits) doesn't produce evident effects. Also span length effects on the beams deflection is important and must not be neglected.

Function	SSE (m^2/s^2)	R-square	AR-square	RMSE (m/s)
Quartic P.Load	368.7	0.41280	0.41020	0.6300
Cubic P.Load	369.5	0.41150	0.40960	0.6303
Quadratic P.Load	370.0	0.41070	0.40950	0.6304
Linear P.Load	371.5	0.40830	0.40770	0.6314
Quartic Slend	527.8	0.15930	0.15570	0.7538
Cubic Slend	528.7	0.15790	0.15520	0.7540
Quadratic Slend	532.2	0.15240	0.15050	0.7561
Linear Slend	542.6	0.13580	0.13490	0.7630
Linear Span	627.8	0.00015	-0.00093	0.8207
Quadratic Span	627.4	0.00068	-0.00147	0.8209
Cubic Span	627.0	0.00137	-0.00185	0.8211
Quartic Span	627.0	0.00141	-0.00289	0.8215

Table 4 : Fitting performances for high-load maximum velocity results.

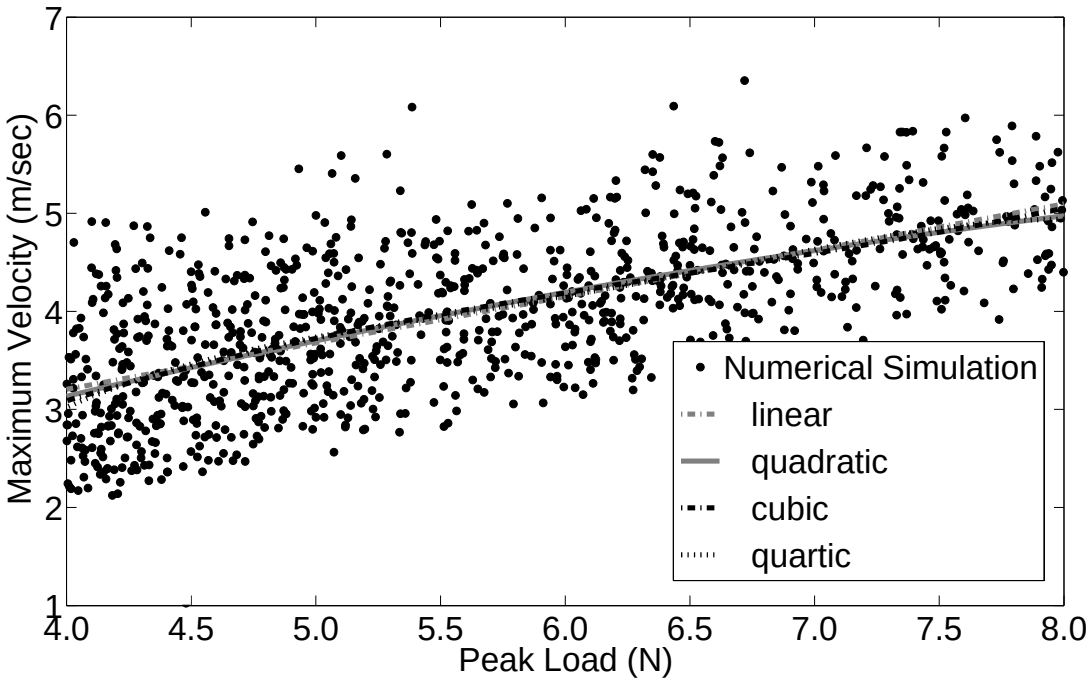

Fig. 12: High Load, Max. Vel. – Peak Load: different kinds of polyn. fittings.

Please cite this document as: STOCHINO F. "RC beams under blast load: Reliability and sensitivity analysis", *Engineering Failure Analysis*, (2016) 66, 544-565. http://dx.doi.org/10.1016/j.engfailanal.2016.05.003 - © 2016. this manuscript version is made available under the CC-BY-NC-ND 4.0 license

Table 4 reports the fitting performance of the correlation between maximum velocities obtained by the SDOF model and the above-mentioned structural parameters in the case of high load. The variation of span length is not significant in this case: AR-square values are always negative and SSE values are high. Better (but still not very significant) results are obtained for the correlation between maximum velocity and slenderness. Considering the latter parameter, SSE values are lower but still high. In Fig. 12, the correlation between maximum velocity and peak load is depicted; SSE values are quite low, and AR-square attains better values than in previous cases. Therefore, for beams under high load condition the best model concerning maximum velocity seems to be a quartic polynomial function of the peak load.

Function	SSE (m^2)	R-square	AR-square	RMSE (m)
Cubic Slend	1.546	0.4629	0.4621	0.02876
Quartic Slend	1.546	0.4630	0.4619	0.02877
Quadratic Slend	1.549	0.4621	0.4615	0.02878
Linear Slend	1.554	0.4601	0.4599	0.02882
Quartic P.Load	2.279	0.2085	0.2068	0.03493
Quadratic P.Load	2.285	0.2064	0.2056	0.03496
Cubic P.Load	2.284	0.2069	0.2056	0.03496
Linear P.Load	2.358	0.1811	0.1807	0.03550
Quartic Span	2.579	0.1044	0.1025	0.03715
Cubic Span	2.586	0.1018	0.1004	0.03720
Linear Span	2.601	0.09676	0.09627	0.03728
Quadratic Span	2.600	0.09688	0.09591	0.03729

Table 5: Fitting performances for low-load maximum deflection results.

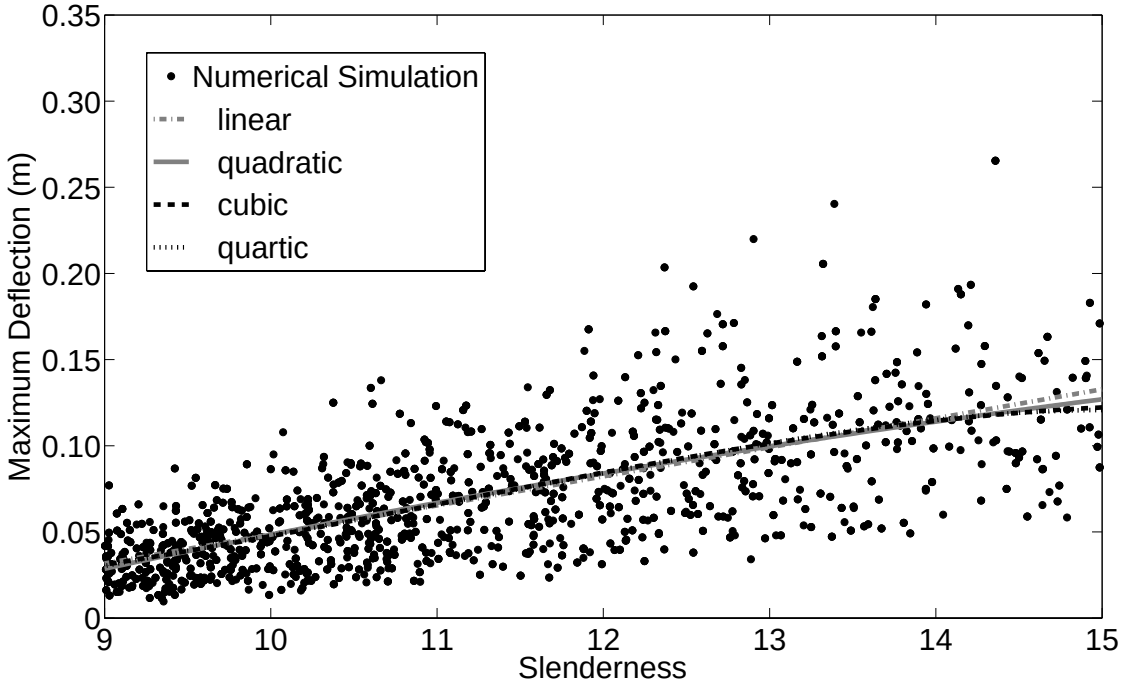

Fig. 13: Low Load, Max. Def. – Slenderness: different kinds of polyn. fittings.

The fitting performances of correlations between maximum deflection (reached by the SDOF during numerical simulations in the case of low load) and span length, slenderness and peak load

Please cite this document as: STOCHINO F. "RC beams under blast load: Reliability and sensitivity analysis", *Engineering Failure Analysis*, (2016) 66, 544-565. http://dx.doi.org/10.1016/j.engfailanal.2016.05.003 - © 2016. this manuscript version is made available under the CC-BY-NC-ND 4.0 license

are presented in Table 5. From the analysis of SSE and AR-square indexes, best fits are obtained, considering slenderness as an independent variable (see Fig. 13). In particular, the cubic function produces the highest AR-square and lowest deviation expressed by quite low SSE and RMSE.
Considering span length and peak load functions, SSE tends to decrease slightly as the number of model coefficients increases, but fitting is always worse than in the previous case. Thus, in accordance to what happened for the high load condition, for the maximum deflection the key parameter seems to be the slenderness.

Function	SSE (m^2/s^2)	R-square	AR-square	RMSE (m/s)
Quartic P.Load	368.7	0.41280	0.41020	0.6300
Cubic P.Load	369.5	0.41150	0.40960	0.6303
Quadratic P.Load	370.0	0.41070	0.40950	0.6304
Linear P.Load	371.5	0.40830	0.40770	0.6314
Quartic Slend	527.8	0.15930	0.15570	0.7538
Cubic Slend	528.7	0.15790	0.15520	0.7540
Quadratic Slend	532.2	0.15240	0.15050	0.7561
Linear Slend	542.6	0.13580	0.13490	0.7630
Linear Span	627.8	0.00015	-0.00093	0.8207
Quadratic Span	627.4	0.00068	-0.00147	0.8209
Cubic Span	627.0	0.00137	-0.00185	0.8211
Quartic Span	627.0	0.00141	-0.00289	0.8215

Table 6: Fitting performances for low-load maximum velocity results.

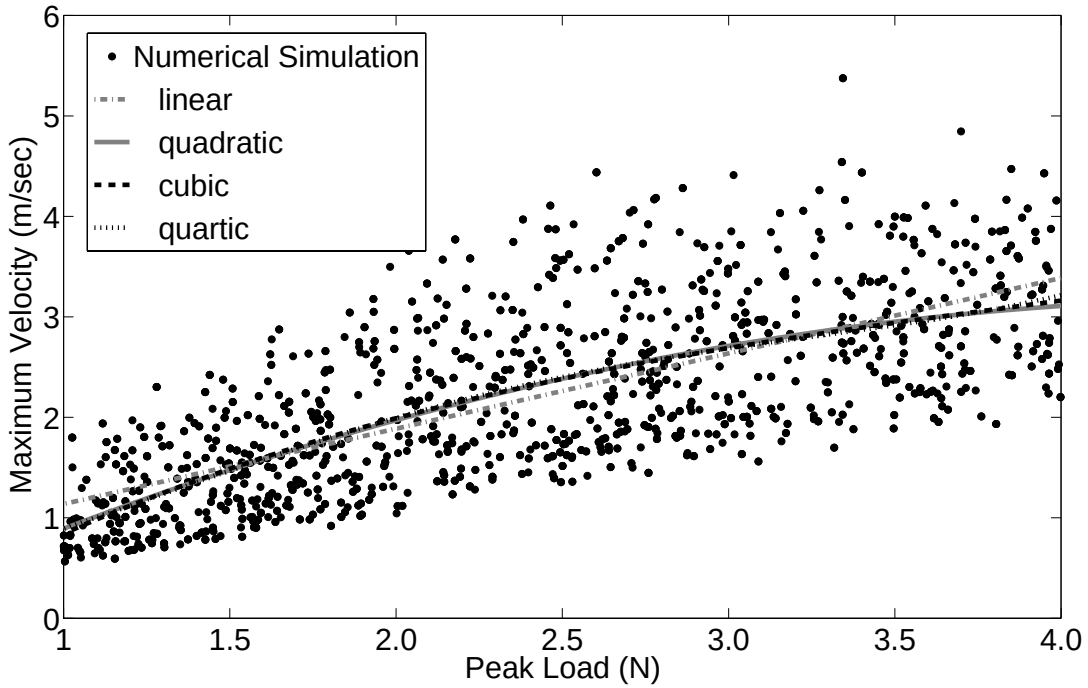

Fig. 14: Low Load, Max. Veloc.– Peak Load: different kinds of polyn. fittings.

Table 6 presents the fitting performance of the correlations between the maximum velocity, obtained in the case of low load, and slenderness, span length and peak load. Similarly to what happened in high load condition, the best correlation is obtained considering peak load (see Fig. 14). Indeed, this is the case with the highest variation index (R-square and AR-square) and lowest

Please cite this document as: STOCHINO F. "RC beams under blast load: Reliability and sensitivity analysis", *Engineering Failure Analysis*, (2016) 66, 544-565. http://dx.doi.org/10.1016/j.engfailanal.2016.05.003 - © 2016. this manuscript version is made available under the CC-BY-NC-ND 4.0 license

deviation index (SSE, RMSE). In particular, the quartic polynomial function produces the best fitting. Correlation between maximum velocity and span length seems not effective, and corresponding fittings obtained poor results. Better results are obtained considering the relationship between maximum velocity and slenderness. In this case as well, SSE decreases as the number of model coefficients increases, and the AR-square increases as the degree of the fitting polynomial increases.

4.2 Three-dimensional relationships

variable	mean	Standard Deviation
Slenderness	10.08	0.7963
P.Load	$0.5575 \cdot 10^6$ N	$0.1109 \cdot 10^6$ N
Span	9.167 m	1.669 m
C.Strength	30.26 MPa	2.837 MPa
R.Ratio	0.0076	0.0014

Table 7 : Mean and standard deviation of the parameters considered for high-load analysis.

variable	mean	Standard Deviation
Slenderness	11.27	1.579
P.Load	$0.2419 \cdot 10^6$ N	$0.0845 \cdot 10^6$ N
Span	9.071 m	1.668 m
C.Strength	30.12 MPa	2.85 MPa
R.Ratio	0.0075	0.0014

Table 8 : Mean and standard deviation of the parameters considered for low-load analysis.

In this paragraph, correlations between maximum displacement (deflection) or velocity and some load and structural parameters are investigated in a three-dimensional space. In this way the joint effect of two parameters can be studied. The dependent variable, *z*, is assumed to be the maximum deflection or the maximum velocity and the independent ones, *x* and *y*, represent the other parameters (peak load, slenderness, span, concrete strength, reinforcement ratio). In the following the notation $poly_{ij}$ denotes a complete polynomial with i-th degree for the *x* and j-th degree for the *y*. Several least squares fitting functions have been compared in order to determine best fitting of the SDOF numerical results. In order to avoid badly conditioned equations, independent variables are normalised by their mean and standard deviation (see Table 7 and Table 8).

Considering the case of high load a synthesis of the fitting performance of maximum displacement results is presented in Table 9, where the lowest SSE is obtained by a 5^{th} degree polynomial function of span length and slenderness (see Fig. 15). This function also presents the best AR-square index. This leads to the conclusion that peak load influence is less important than span length as regards maximum deflection in the case of a high load. As described in Section 4.1, this can be explained by the fact that the variation range of peak load for this analysis is very narrow (indeed only a few number of beams withstood the load) and so it does not have a strong correlation with results variations.

From Table 9, it is clear that concrete strength and reinforcement ratio have not a strong correlation with maximum deflection. This can be explained considering that the SDOF model failure condition cannot allow to represent the damage propagation along the beam and the effects of this two variable on the deflection may become important beyond the ultimate limit condition considered in this work.

Please cite this document as: STOCHINO F. “RC beams under blast load: Reliability and sensitivity analysis”, *Engineering Failure Analysis*, (2016) 66, 544-565. http://dx.doi.org/10.1016/j.engfailanal.2016.05.003 - © 2016. this manuscript version is made available under the CC-BY-NC-ND 4.0 license

Actually, as mentioned above, functions of span length and slenderness present lower fitting errors and it is important to underline how it is possible to have good fit even with a simple cubic function (see Fig. 16).

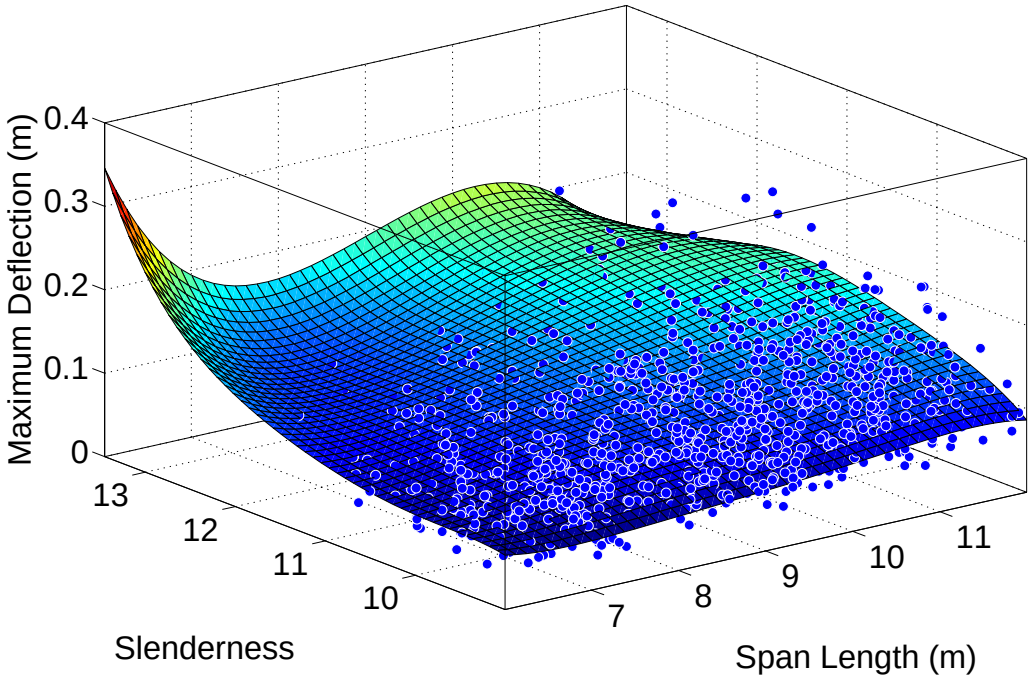

Fig. 15: High Load, Max Deflection, Slenderness - Span 5th deg. polyn. fitting.

x – y	Fit type	SSE m^2	R-SQUARE	AR-SQUARE	RMSE m	Coefficients
Span –Slend.	$poly_{55}$	0.599829	0.551294	0.541454	0.025646	21
Slend- P.Load	$poly_{55}$	0.601113	0.550334	0.540473	0.025673	21
Span-Slend.	$poly_{44}$	0.604141	0.548069	0.541177	0.025654	15
Slend- P.Load	$poly_{44}$	0.605854	0.546787	0.539876	0.025690	15
Span-Slend.	$poly_{33}$	0.606089	0.546612	0.542191	0.025625	10
Span-Slend.	$poly_{22}$	0.606666	0.546180	0.543733	0.025582	6
Slend- P.Load	$poly_{33}$	0.60937	0.544157	0.539712	0.025694	10
Slend- P.Load	$poly_{22}$	0.613641	0.540963	0.538487	0.025729	6
Span-Slend.	$poly_{44}$	0.618171	0.541562	0.534578	0.025936	15
Slend- P.Load	$poly_{11}$	0.629505	0.529095	0.528083	0.026017	3
Span-Slend.	$poly_{11}$	0.633605	0.526028	0.525009	0.026102	3
Slend- R.Ratio	$poly_{55}$	0.664026	0.507555	0.496768	0.026969	21
Span- P.Load	$poly_{55}$	0.846643	0.372126	0.358372	0.030452	21
Slend.-C.Stren.	$poly_{55}$	0.938409	0.304072	0.288827	0.032060	21

Table 9 : Fitting performances for high-load maximum deflection results considering different parameters as independent variables *x*, *y*. For each case the fitting performance indicator, presented in Section 3.3, and the number of the polynomial coefficients are reported.

Table 10 represents a synthesis of fitting performances in the case of high load, considering maximum velocity as dependent variable. The lowest SSE is obtained by a 5th degree polynomial

Please cite this document as: STOCHINO F. "RC beams under blast load: Reliability and sensitivity analysis", *Engineering Failure Analysis*, (2016) 66, 544-565. http://dx.doi.org/10.1016/j.engfailanal.2016.05.003 - © 2016. this manuscript version is made available under the CC-BY-NC-ND 4.0 license

function of slenderness and peak load. The best AR-square index corresponds to a 3rd degree polynomial function of the same variables, see Fig. 17. From these results, it is clear that the most important parameters fitting maximum velocity/high load results are peak load and slenderness. Other variables functions obtained dramatically worse results. Finally, it is interesting to underline the importance of the peak load, whose functions occupy the first seven positions in Table 10. Actually, the slenderness function produces lower fitting performance. These observations confirm what was stated in the previous Section 4.1

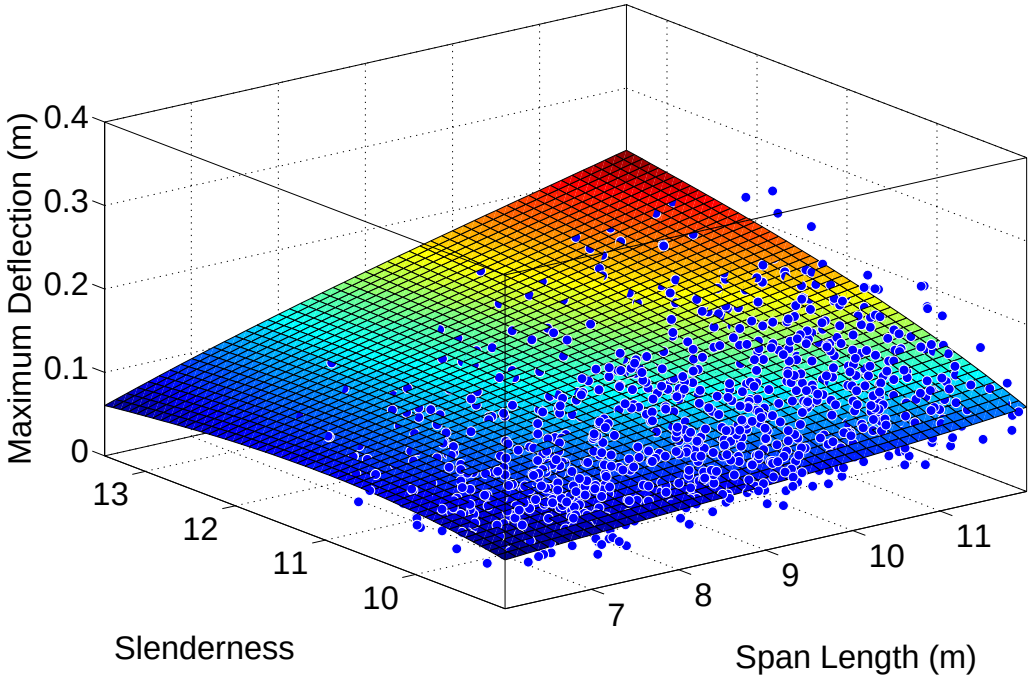

Fig. 16: High Load, Max Deflection, Slenderness - Span 3rd deg. polyn. fitting.

x – y	Fit type	SSEm²/sec²	R-SQUARE	AR-SQUARE	RMSE m/sec	Coefficients
Slend.-P.Load	$poly_{55}$	91.67459508	0.851965086	0.848718707	0.317049506	21
Slend.-P.Load	$poly_{44}$	92.23189316	0.851065169	0.848793832	0.316970774	15
Slend.-P.Load	$poly_{33}$	92.49950564	0.850633032	0.849176583	0.316569343	10
Slend.-P.Load	$poly_{22}$	92.92596403	0.849944393	0.849135031	0.316612947	6
Slend.-P.Load	$poly_{11}$	98.40803253	0.841092021	0.840750284	0.325292313	3
P.Load.-C.Stren.	$poly_{33}$	357.6543056	0.422464597	0.416833157	0.622487849	10
P.Load – Span.	$poly_{33}$	362.5423019	0.414571526	0.408863122	0.626727128	10
Slend.-Span	$poly_{55}$	508.139387	0.179463294	0.161469068	0.746438464	21
Slend.-Span	$poly_{44}$	510.7910993	0.175181345	0.162602411	0.745933857	15
Slend.-C.Stren.	$poly_{33}$	511.2570454	0.174428941	0.166378952	0.74424993	10
Slend.-Span	$poly_{33}$	512.3703241	0.172631233	0.164563716	0.745059803	10
Slend.-Span	$poly_{22}$	515.5991811	0.167417318	0.162926581	0.745789462	6
Slend.-Span	$poly_{11}$	529.3251071	0.145252876	0.14341471	0.75443143	3

Table 10: Fitting performance for high-load maximum velocity results, considering different parameters as independent variables *x*, *y*. For each case the fitting performance indicator, presented in Section 3.3, and the number of the polynomial coefficients are reported.

Please cite this document as: STOCHINO F. "RC beams under blast load: Reliability and sensitivity analysis", *Engineering Failure Analysis*, (2016) 66, 544-565. http://dx.doi.org/10.1016/j.engfailanal.2016.05.003 - © 2016. this manuscript version is made available under the CC-BY-NC-ND 4.0 license

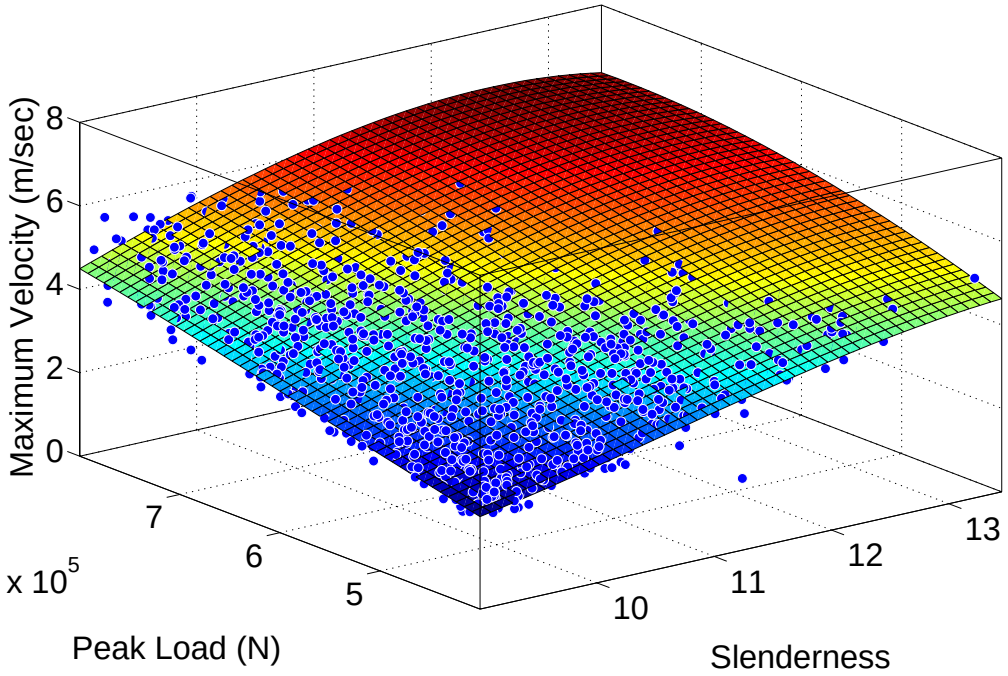

Fig. 17: High Load, Max. Velocity, Peak Load - Slenderness 5th polyn. fitting.

x – y	Fit type	SSE m^2	R-SQUARE	AR-SQUARE	RMSE m	Coefficients
Slend.-P.Load	$poly_{55}$	0.58467087	0.796950663	0.794757906	0.017767865	21
Slend.-P.Load	$poly_{44}$	0.591579941	0.794551224	0.793003171	0.017843657	15
Slend.-P.Load	$poly_{33}$	0.59624080	0.792932562	0.791932236	0.017889756	10
Slend.-P.Load	$poly_{22}$	0.601406477	0.791138583	0.790579233	0.017947828	6
Slend.-P.Load	$poly_{11}$	0.75360261	0.738282651	0.738002739	0.020074761	3
Slend.-Span	$poly_{55}$	1.249337712	0.566119663	0.561434130	0.02597284	21
Slend.-Span	$poly_{44}$	1.255508783	0.563976523	0.560691093	0.025994832	15
Slend.-Span	$poly_{33}$	1.264076134	0.561001182	0.558880415	0.026048348	10
Slend.-Span	$poly_{22}$	1.265849822	0.560385201	0.559207872	0.026038678	6
Slend.-Span	$poly_{11}$	1.327557523	0.53895484	0.538461744	0.026644395	3
P.Load-R.Ratio	$poly_{11}$	2.128770294	0.260703041	0.259912349	0.033739885	3
C.Stren.-P.Load	$poly_{11}$	2.351506343	0.183349423	0.182476000	0.035461106	3

Table 11: Fitting performance for low-load maximum deflection results, considering different parameters as independent variables *x*, *y*. For each case the fitting performance indicator, presented in Section 3.3, and the number of the polynomial coefficients are reported.

The case of low-load has been analysed considering as dependent variable the maximum displacement and the maximum velocity. If we consider the former case a synthesis of the analysis

is shown in Table 11: the lowest SSE is obtained by a 5th degree polynomial function of slenderness and peak load (see Fig. 18). This function also presents the best AR-square index. These results underline the importance of peak load and slenderness in the estimation of beam response under blast load.

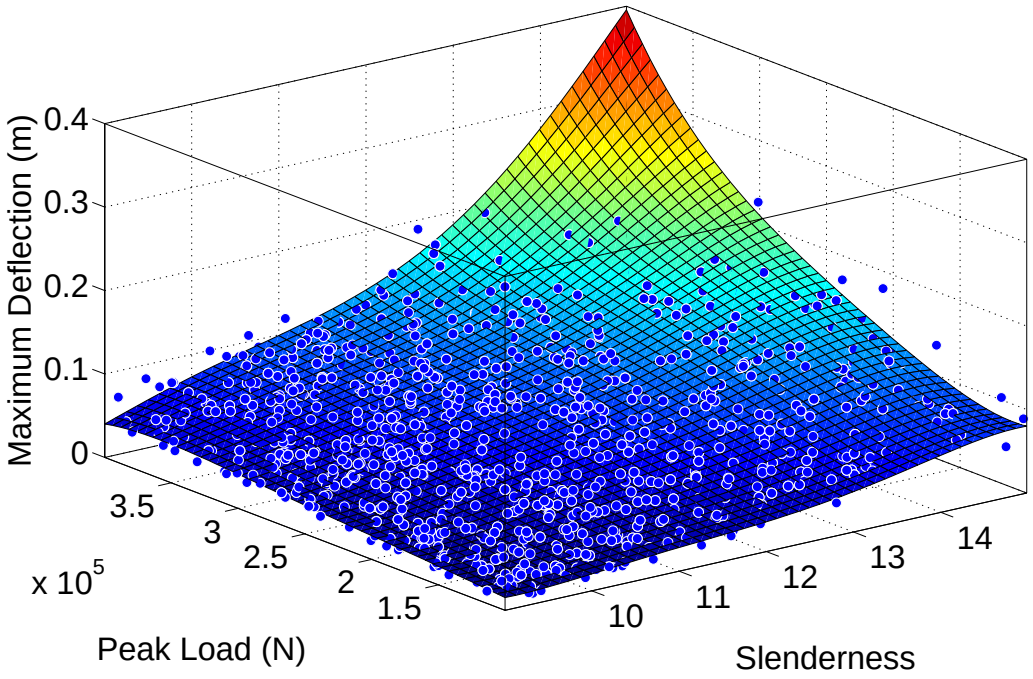

Fig. 18: Low Load, Max. Deflection, Peak Load - Slenderness 5th polyn. fitting.

x – y	Fit type	SSE m²/sec²	R-SQUARE	AR-SQUARE	RMSE m/sec	Coefficients
Slend.-P.Load	$poly_{55}$	74.15608153	0.951244314	0.950717795	0.200102675	21
Slend.-P.Load	$poly_{44}$	74.91211988	0.950747238	0.95037612	0.200795136	15
Slend.-P.Load	$poly_{33}$	75.21087461	0.950550815	0.95031193	0.200924961	10
Slend.-P.Load	$poly_{22}$	75.41919317	0.950413851	0.950281055	0.200987377	6
Slend.-P.Load	$poly_{11}$	132.1395093	0.913121725	0.913028807	0.265824828	3
Slend.-Span	$poly_{55}$	1026.960884	0.324800050	0.317508474	0.744657315	21
Slend.-Span	$poly_{44}$	1031.492396	0.321820699	0.316710629	0.745092446	15
Slend.-Span	$poly_{33}$	1038.129148	0.317457208	0.314159900	0.746481871	10
Slend.-Span	$poly_{22}$	1038.440420	0.317252555	0.315424094	0.745793567	6
R.Ratio-Slend.	$poly_{11}$	1054.338630	0.306799897	0.306058507	0.750877786	3
Slend.-Span	$poly_{11}$	1073.179019	0.294412834	0.293658195	0.757556944	3
C.Stren.-Slend.	$poly_{11}$	1076.444277	0.292266012	0.291509077	0.758708542	3

Table 12: Fitting performance for low-load maximum velocity results, considering different parameters as independent variables *x*, *y*. For each case the fitting performance indicator, presented in Section 3.3, and the number of the polynomial coefficients are reported.

Please cite this document as: STOCHINO F. "RC beams under blast load: Reliability and sensitivity analysis", *Engineering Failure Analysis*, (2016) 66, 544-565. http://dx.doi.org/10.1016/j.engfailanal.2016.05.003 - © 2016. this manuscript version is made available under the CC-BY-NC-ND 4.0 license

Table 12 presents a synthesis of the fitting performance in case of low load, considering velocity as a dependent variable. Also in this situation the lowest SSE is obtained by a 5th degree polynomial function of slenderness and peak load (see Fig. 19). The same function obtains the best AR-square index. From these results, it is clear that the most important parameters for fitting maximum velocity/low load results are peak load and slenderness. Other variables obtained dramatically worse results. Actually, a simple linear function of peak load and slenderness fits the numerical results better than more sophisticated functions of other variables (i.e. the 5th degree polynomial corresponding to slenderness and span length).

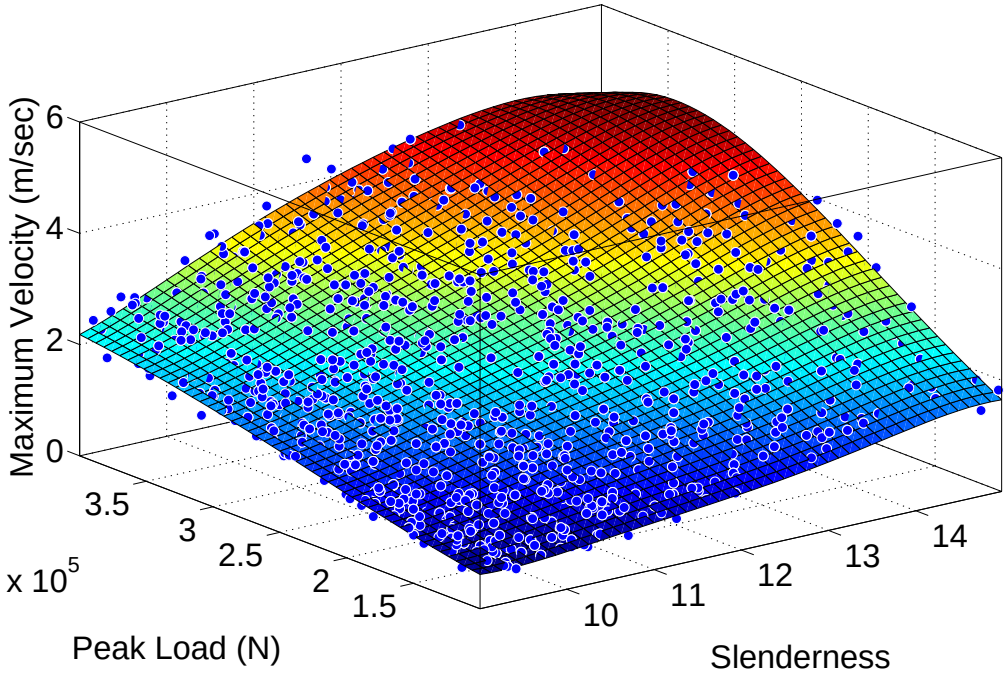

Fig. 19: Low Load, Max. Velocity, Peak Load - Slenderness 5th polyn. fitting.

5 Conclusions

This paper has presented a reliability and parametric analysis of the structural response of Reinforced Concrete beams under blast loads. The main aim was to highlight the key parameters of the problem in order to produce information useful for the design of reliable blast-resistant structures.

The beam has been idealised as an equivalent SDOF system, in which strain-rate effects are accounted for. This approach is convenient from a computational point of view and it has been validated by a direct comparison with experimental results found in literature and with a more sophisticated FE model.

First a huge number of SDOF numerical simulation had been employed for the reliability analysis. As a result, Fig. 9 was obtained. It presents the percentage of collapsed beam as a function of peak load and slenderness. So it can give a rough measure of reliability for the given combination of peak load and slenderness. Then a sensitivity analysis of the parameters involved in beam response under blast load has been developed. Results of numerical simulations obtained by means of the SDOF model in terms of deflection and velocity have been fitted by proper polynomial least-square

Please cite this document as: STOCHINO F. "RC beams under blast load: Reliability and sensitivity analysis", *Engineering Failure Analysis*, (2016) 66, 544-565. http://dx.doi.org/10.1016/j.engfailanal.2016.05.003 - © 2016. this manuscript version is made available under the CC-BY-NC-ND 4.0 license

interpolation. Random variations of beams and load characteristics have been considered. Among the various fitting functions of several parameters (peak load, positive phase duration, slenderness, span length, concrete strength, reinforcement ratio etc.) slenderness and peak load prove to be the most important parameters, but span is also a key parameter. Actually, given the slenderness the span length corresponds to the mass of the beam and, in impulsive load regime, it is crucial to determine the initial velocity which is equal to the ratio between impulse and the mass itself. Furthermore, the slenderness is strictly linked to the beam flexural stiffness which is the only elastic term in the Euler-Bernoulli beam equation and the peak load is a key parameter to identify the load. Other variables such as concrete strength and reinforcement ratio do not seem to have a high correlation with the beam response within the limits of the SDOF model.

The latter approach can be very suitable for early analysis in the case of blast-resistant structural design. Indeed a first indication of what slenderness is necessary to withstand the load can be obtained looking at Fig. 9. In addition, the above presented fitting functions can be translated in suitable tables where it is possible to find the maximum deflection (see Table 13) or maximum velocity of a beam with a given slenderness under a given blast load characterized by a given peak value. These tables can also be calculated for different loads, boundary conditions, failure criterions and for other different significant parameters. Moreover, instead of a random variation of the variables accounted in this section, it would be interesting to consider other typical distribution functions such as the Gauss-normal or a Fuzzy representation.

Slenderness\Peak Load	**$4{\cdot}10^5$ N**	**$5{\cdot}10^5$ N**	**$6{\cdot}10^5$ N**	**$7{\cdot}10^5$ N**	**$8{\cdot}10^5$ N**
9	0.044	0.061	0.079	0.097	0.114
10	0.079	0.096	0.114	0.131	0.149
11	0.114	0.131	0.149	0.166	0.184
12	0.149	0.166	0.184	0.201	0.219
13	0.184	0.201	0.219	0.236	0.254
14	0.218	0.236	0.254	0.271	0.289
15	0.253	0.271	0.288	0.306	0.324

Table 13: High Load – Maximum Displacement estimation (in meter) based on the poly 1-1 model Slenderness/Peak Load. The black thick line identifies the conditions in which the percentage of collapse exceeds 50%.

6 References

[1] A. Sorensen, W. L. Mc Gill, What to look for in the aftermath of an explosion? A review of blast scene damage observables, Eng. Fail. Anal., 18 (2011) 836-845.

[2] W. Wang, R. Liu, B. Wu, Analysis of a bridge collapsed by an accidental blast loads, Eng. Fail. Anal., 36 (2014) 353-361.

[3] J. M. Frankland, Effects on Impact of Simple Elastic Structures, Taylor Model Basin Report No. 481, April, 1942.

[4] C. M. Morison, Dynamic response of walls and slabs by single-degree-of-freedom analysis—a critical review and revision. Int. J. Impact Eng., 32 (2006) 1214–1247.

[5] Fundamentals of protective design (Non-nuclear) TM 5-855-1. Washington, DC: Department of the Army; March 1965. (Reprint of former document 1110-345-405, 1946).

[6] J.A. Seiler, B.A. Cotter, P.S. Symonds, R.I. Providence, Impulsive Loading of Elastic-

Please cite this document as: STOCHINO F. “RC beams under blast load: Reliability and sensitivity analysis”, *Engineering Failure Analysis*, (2016) 66, 544-565. http://dx.doi.org/10.1016/j.engfailanal.2016.05.003 - © 2016. this manuscript version is made available under the CC-BY-NC-ND 4.0 license

Plastic Beams. J. Appl. Mech. 23 (1956) 515-521.
[7] N.B. Brooks, N.M. Newmark, The response of simple structures to dynamic loads, Technical report to ONR contract N6ori-071(06), Task Order VI Project NR-064-183 University of Illinois Urbana, Illinois, 1953.
[8] N.M. Newmark An engineering approach to blast resistant design, Proc. Am. Soc. Civ. Eng. 79 (1953) 306:1-16.
[9] Design of structures to resist Nuclear weapon effects. ASCE manuals & reports on engineering practice—No. 42. New York: American Society of Civil Engineers; 1961.
[10] Design of structures to resist the effects of atomic weapons—principles of dynamic analysis and design, EM 1110- 345-415. Washington, DC: US Army Corps of Engineers; March 1957.
[11] Design of structures to resist the effects of atomic weapons—principles of structural elements subjected to dynamic loads, EM 1110-345-416, Washington, DC: US Army Corps of Engineers; March 1957.
[12] J.M. Biggs, Introduction to structural dynamics. New York: McGraw-Hill Book Company; 1964.
[13] F. Stochino, G. Carta, SDOF models for reinforced concrete beams under impulsive loads accounting for strain rate effects, Nucl. Eng. Des. 276 (2014) 74–86.
[14] M. Acito, F. Stochino, S. Tattoni, Structural response and reliability analysis of RC beam subjected to explosive loading, App. Mech. Mat. 82 (2011) 434–439.
[15] K. Fischer, I. Häring SDOF response model parameters from dynamic blast loading experiments, Eng. Struct., 31(2009) 1677–1686.
[16] A.A. Nassr, A.G. Razaqpur, M.J. Tait, M. Campidelli, S. Foo, Single and multi degree of freedom analysis of steel beams under blast loading. Nucl Eng Des, 242 (2012) 63-77.
[17] G. Yang,T.S. Lok, Analysis of RC structures subjected to air-blast loading accounting for strain rate effect of steel reinforcement, Int. J. Impact. Eng. 34 (2007) 1924-1935.
[18] A. Cazzani , M. Malagù, E. Turco, and F. Stochino, Constitutive models for strongly curved beams in the frame of isogeometric analysis, Math. Mech. Solids, 21(2), (2016) 182-209.
[19] A. Cazzani, F. Stochino, E. Turco, A computational assessment via Finite Elements and Isogeometric Analysis of the whole spectrum of Timoshenko beams, in press (2016), 1–30, doi: 10.1002/zamm.201500280.
[20] A. Cazzani, F. Stochino, E. Turco, On the whole spectrum of Timoshenko beams. Part I: a theoretical revisitation, Z. Angew. Math. Phys., 67: 24, (2016) 1–30.
[21] A. Cazzani, F. Stochino, E. Turco, On the whole spectrum of Timoshenko beams. Part II: further applications, Z. Angew. Math. Phys. 67: 25, (2016) 1–21.
[22] T. Xu, T. Xiang, R. Zhao, G. Yang, Stochastic analysis on flexural behavior of reinforced concrete beams based on piecewise response surface scheme, Eng. Fail. Anal., 59 (2016): 211-222.
[23] Z. Wen, G. Xiao, X. Jin, M. Zhu, Dynamic vehicle–track interaction and plastic deformation of rail at rail welds, Eng. Fail. Anal. 16.4 (2009) 1221-1237.
[24] G. Carta, F. Stochino, Theoretical models to predict the flexural failure of reinforced concrete beams under blast loads, Eng. Struct., 49 (2013) 306–315.
[25] L.B. Jayasinghe, D.P. Thambiratnam, N. Perera, J.H.A.R. Jayasooriya, Blast response and failure analysis of pile foundations subjected to surface explosion, Eng. Fail. Anal, 39, (2014), 41-54.
[26] B. Yan, F. Liu, D.Y. Song, Z.G. Jiang, Numerical study on damage mechanism of RC beams under close-in blast loading, Eng. Fail. Anal., 51 (2015) 9-19.

Please cite this document as: STOCHINO F. “RC beams under blast load: Reliability and sensitivity analysis”, *Engineering Failure Analysis*, (2016) 66, 544-565. http://dx.doi.org/10.1016/j.engfailanal.2016.05.003 - © 2016. this manuscript version is made available under the CC-BY-NC-ND 4.0 license

[27] C. Naito, P. Olmati, P. Trasborg, J. Davidson, C. Newberry, Assessment of Insulated Concrete Walls to Close-In Blast Demands, J. Perform. Constr. Fac. 29 (2015) art. no. 04014149.
[28] P. Olmati, F. Petrini, F. Bontempi, Numerical analyses for the structural assessment of steel buildings under explosions, Struct. Eng. Mech., 45 (2013) 803-819.
[29] C. Bedon, C. Amadio, Exploratory numerical analysis of two-way straight cable-net façades subjected to air blast loads, Eng. Struct., 79 (2014) 276-289.
[30] C. Bedon, C. Amadio, A. Sinico, Numerical and analytical investigation on the dynamic buckling behavior of glass columns under blast, Eng. Struct., 79 (2014) 322-340.
[31] C. Amadio, C. Bedon, FE assessment of dissipative devices for the blast mitigation of glazing fa çades supported by prestressed cables, Struct. Eng. Mech., 51 (2014) 141-162.
[32] J. Magnusson Structural concrete elements subjected to air blast loading [Licentiate thesis]. TRITA-BKN Bulletin 92. Stockholm (Sweden): Royal Institute of Technology; (2007).
[33] J. Magnusson, M. Hallgren, High performance concrete beams subjected to shock waves from air blast, Report n. FOA-R–00-01586-311–SE, (2000) Defence Research Establishment (FOA), Tumba, Sweden.
[34] J. Magnusson, M. Hallgren, High performance concrete beams subjected to shock waves from air blast, Part 2, Report n. FOI-R–1116–SE, (2003) Swedish Defence Research Agency (FOI), Tumba, Sweden.
[35] J. Magnusson, M. Hallgren, Reinforced high strength concrete beams subjected to air blast loading, In: Jones N, Brebbia CA, editors. Structures under shock and impact VIII. Southampton: WIT, (2004), pp. 53-62.
[36] J. Magnusson, M. Hallgreny, A. Ansell, Air-blast-loaded, high-strength concrete beams. Part I: Experimental investigation, Mag. Concrete Res., 62 (2010) 127-136.
[37] J. Magnusson, A. Ansell, H. Hansson, Air-blast-loaded, high-strength concrete beams. Part II: Numerical non-linear analysis, Mag. Concrete Res., 62 (2010) 235-242.
[38] J.L. Hudson, D. Darwin, Evaluation and repair of blast damaged reinforced concrete buildings. SL Report 05-1, University of Kansas Center for Research, Inc., Lawrence, Kansas, USA; (2005).
[39] A.M. Remennikov, S. Kaewunruen, Impact resistance of reinforced concrete columns: experimental studies and design considerations. Proceedings of the 19th Australasian Conference on the Mechanics of Structures and Materials; 2006 Nov 29 - Dec 1; Christchurch, New Zealand. Tailor & Francis; (2007), p. 817-824.
[40] K. Fujikake, B. Li, S. Soeun, Impact response of reinforced concrete beam and its analytical evaluation, J. Struct. Eng., 135 (2009) 938-950.
[41] T. Zhan, Z. Wang, J. Ning, Failure behaviors of reinforced concrete beams subjected to high impact loading, Eng. Fail. Anal., 56 (2015) 233-243.
[42] S. Tachibana, H. Masuya, S. Nakamura, Performance based design of reinforced concrete beams under impact, Nat Hazards Earth Syst Sci, 10 (2010) 1069-1078.
[43] G. Giovino, P. Olmati, S. Garbati, F. Bontempi, Blast resistance assessment of concrete wall panels: Experimental and numerical investigations, Int. J. Protect. Struct., 5 (2014) 349-366.
[44] W. Wang, D. Zhang, F. Lu, S. Wang, F. Tang, Experimental study and numerical simulation of the damage mode of a square reinforced concrete slab under close-in explosion, Eng. Fail. Anal., 27 (2013) 41-51.
[45] R. Codina, D. Ambrosini, F. de Borbón, Alternatives to prevent the failure of RC

members under close-in blast loadings, Eng. Fail. Anal., 60, (2016), 96-106.

[46] D. Zhang, S.J. Yao, F. Lu, X.G. Chen, G. Lin, W. Wang, Y. Lin, Experimental study on scaling of RC beams under close-in blast loading, Eng. Fail. Anal., 33 (2013) 497-504.

[47] H.Y. Low., H. Hao, Reliability analysis of reinforced concrete slabs under explosive loading. Structural Safety 23 (2001) 157–178.

[48] H.-C. Rong and B. Li, Probabilistic response evaluation for RC flexural members subjected to blast loadings. Structural Safety 29 (2007) 146–163.

[49] M. A. Smith, L. Caracoglia, A Monte Carlo based method for the dynamic "fragility analysis" of tall buildings under turbulent wind loading, Eng. Struct., 33 (2011) 410-420.

[50] E. Borenstein., H. Benaroya, Sensitivity analysis of blast loading parameters and their trends as uncertainty increases. J. Sound Vib., 321 (2009) 762–785.

[51] P. Olmati, P. Trasborg, C. Naito, F. Bontempi, Blast resistant design of precast reinforced concrete walls for strategic infrastructures under uncertainty, Int. J. Crit. Infrastruct., 11 (2015) 197-212.

[52] F. Parisi, Blast fragility and performance-based pressure-impulse diagrams of European reinforced concrete columns, Eng. Struct., 103 (2015) 285-297.

[53] P. Olmati, F. Petrini, K. Gkoumas, Fragility analysis for the Performance-Based Design of cladding wall panels subjected to blast load, Eng. Struct., 78 (2014) 112-120.

[54] Federal Institute of Technology. Model Code 2010, First Complete Draft, Volume 1. Lausanne (Switzerland): fib Bulletin 55; 2010.

[55] Comité Euro-International du Béton. Concrete structures under impact and impulsive loading. Lausanne (Switzerland): CEB Bulletin 187; 1988.

[56] W. Riedel, K. Fischer, C. Kranzer, J. Erskine, R. Cleave, D. Hadden, M. Romani, Modeling and validation of wall-window retrofit system under blast loading, Eng Struct, 37 (2012) 235-245.

[57] H. Mattock, Discussion of 'rotational capacity of reinforced concrete beams', J. Struct. Div., 93ST2 (1967) 519–522.

[58] A. Marini, E. Spacone, Analysis of reinforced concrete elements including shear effects. ACI Struct.l J. 103.5 (2006): 645-655.

1

Please cite this document as: STOCHINO F. "RC beams under blast load: Reliability and sensitivity analysis", *Engineering Failure Analysis*, (2016) 66, 544-565. http://dx.doi.org/10.1016/j.engfailanal.2016.05.003 - © 2016. this manuscript version is made available under the CC-BY-NC-ND 4.0 license